Application of the Reactivity Method on KSU TRIGA Fuel

by

Saqr Mofleh Alshogeathri

B.S., Kansas State University, 2013

A Thesis

submitted in partial fulfillment of the requirements for the degree

Master of Science

Department of Mechanical and Nuclear Engineering

College of Engineering

Kansas State University

Manhattan, Kansas

2017

Approved by:

Major Professor

Jeremy Roberts

Abstract

The reactivity method is an indirect nondestructive technique to estimate integral burnup in fuel elements. In this method, the assumption is made that reactivity worth of a fuel element is a known function of burnup, often a linear relationship. When a fuel element burns, reactivity is reduced due to depletion of fissile actinides and generation of neutron-absorbing fission products. Currently, there is a lack of experimental data to verify the current composition of the KSU TRIGA (Training Research Isotopes General Atomics) fuel. Moreover, the KSU TRIGA Mark II staff method of estimating burnup is admittedly inaccurate due to its simple approximations. This work presents the positive period technique as convenient method use only the excess reactivity of the KSU core to compute reactivity via the inhour equation. Period measurements are determined via extraction and manipulation of the time dependent power data in the measurements. MCNP and Serpent modeling codes are both used extract the neutron kinetics parameters necessary in the inhour equation. Seven axial discretization of the KSU fuel was modeled, which minimizes the reactivity biases as function of burnup. Moreover, two unit cell models of the KSU TRIGA fuel were investigated. Modeled reactivity worths were computed using the KCODE in MCNP for comparative analysis. The burnup steps using two power peaking factor methods were developed to account for the biases introduced initial burnup of fuel prior to installation at KSU. By using the error distribution given by the two method to generate 200 test cases of the burnup steps can yield to reactivity worths as a function of burnup with quantifiable uncertainties. Finally, the results suggest that validation from another nondestructive technique such as gamma spectroscopy is necessary to asses the reactivity biases observed for higher burnup fuel elements due to unknown radial orientations. This work ultimately supports the production of a high-fidelity model of the KSU reactor.

Table of Contents

List of Figures

List of Tables

List of Abbreviations

AEC	**A**tomic **E**nergy **C**ommission
CERCA	**C**ompagnie pour l'**E**tude et la **R**éalisation de **C**ombustibles **A**tomiques
FLIP	**F**uel **L**ifetime **I**mprovement **P**rogram
HEU	**H**igh **E**nriched **U**ranium
KSU	**K**ansas **S**tate **U**niversity
LEU	**L**ow **E**nriched **U**ranium
MWD	**M**ega **W**att **D**ay
NMP	**N**uclear **M**ulit-range **P**ower
NLW	**N**uclear **L**ogarithmic **W**ide-range
NPP	**N**uclear **P**ercent **P**ower
PRKE	**P**oint **R**eactor **K**inetics **E**quation
RO	**R**eactor **O**perator
SRO	**S**enior **R**eactor **O**perator
SS	**S**tainless **S**teel
TRIGA	**T**raining **R**esearch **I**sotopes **G**eneral **A**tomics

Acknowledgements

I thank God first and foremost for the blessings and opportunities that he has bestowed upon me and giving me the ability to make this thesis possible. I would like to take time to thank a few of those that have helped me accomplish this goal. First, my special thanks go to my parents Mofleh and Ghozyel Alshogeathri for their unconditional love and support. Without their patience and sacrifices, I would not have been able to be where I am today. My debt to them is unending. I would also like to time to thank those who have shared this journey in shaping this work. First, my sincere gratitude goes to my advisor Professor Jeremy Roberts. His guidance and encouragement along the way made me a better researcher and showed me by example the value of work ethic. I am honored and privileged to have worked closely with him. I would like to also express my special thanks to my mentor throughout my undergraduate and graduate career, Dr. Jeffrey Geuther. I am honored to have worked under him as a staff member of the KSU TRIGA Mark II reactor and will always be in dept for the time he has made for me in answering my questions and concerns. I would like to express my appreciation to Professor William Dunn for serving on my thesis committee. His kindness and invaluable comments have improved my thesis, and so for that I thank him. I would like to also thank the faculty members and staff at the Mechanical and Nuclear department for who have shaped my knowledge in the field that I love so much. In addition, I would like to thank my undergraduate advisor Dr. Ali Abdou who first introduced me to Nuclear Engineering and has been a steadfast advisor over the years.

It is impossible to mention each person who has shared this tremendous journey with me, however there are a few who deserve special recognition. First, I would like to thank my brothers Ali and Ahmed, and my cousin Muhannad Alshogeathri for their help, support, care, and concern. They constantly remind me how grateful I am for having them as brothers. I would like to express my thanks to my wonderful sisters Norah, Sarah, Dalal and baby brother Mohammed for their love that lifted my spirit when I needed it. I extend my appreciation to my grandmother Norah and my great-aunt Sarah for their wisdom and prayers during the completion of my studies. I would like to thank my friends for the interesting years we have spent together in Manhattan, KS; Abdullah Alyami, Ali Alyami, Abdullah Alhakbani, Adeeb Alqahtani, and Musaad Majrishi. I would like to take time to thank as well my friends Max Nager and Sarah Stevenson for the many precious times we spent

together in Ward Hall. I would like to express my thanks also to the rest of the staff members: Joe Hewitt, Max Langston, Robert Seymour, David Van Ommen, Dan Nichols, and Stuart Kern who have helped me with the setup of this work. I would like to thank my collegue and friend Richard Reed who was nothing but gracious with his time in helping when I needed it. I would like to express my thanks to my colleagues Kevin, Ye, and Rabab who have supported not only the content of my work but also their support in finishing my thesis.

I would like to acknowledge the NRC for its support of this work and the Saudi Arabian Culture Mission (SACM), without which this work would not have been possible.

Dedication

To seekers of knowledge

Chapter 1

Introduction

1.1 Overview

Initial efforts have been made at Kansas State University (KSU) to produce a high-fidelity computer-based model of the KSU TRIGA (Training Research Isotopes General Atomics) Mark II reactor. Developing such a model requires a combination of theoretical analysis, reactor operational history, and experimental data. Moreover, a detailed model of the KSU reactor requires that the present core composition be precisely defined with well-understood uncertainties. The KSU TRIGA reactor is fueled with TRIGA MARK III fuel designed by General Atomics (GA) to have a very small critical mass of uranium coupled with a zirconium hydride moderator; see Chapter 2 for description of the fuel. Historical inventories of KSU TRIGA fuel include little information on the initial fuel composition due to depletion prior to insertion into the KSU reactor. Additionally, there exists a lack of experimental data to verify the present composition. The present core composition depends strongly on the initial and subsequent fuel loadings and irradiation history, and thus a detailed accounting of material evolution over time is strongly needed. While this presents a challenge in developing the model, it also presents an opportunity to generate new benchmark data suitable for the effort. To address the data needed, efforts were made to understand the nondestructive

techniques and computational tools available to quantify burnup of fuel elements irradiated in the KSU reactor. Burnup is a process when nuclear fuel undergoes significant compositional changes due to depletion of the isotopes. During its time in the reactor, the fuel "burns," ultimately depleting the most important isotope ^{235}U and generating various fission products. Some of these fission products are parasitic neutron absorbers, e.g., stable ^{149}Sm and radioactive ^{135}Xe. Each spent fuel element contains several hundred different isotopes, the concentrations of which vary considerably in the axial dimension, and potentially, in the radial and azimuthal dimensions.

Gamma spectroscopy is one nondestructive technique used to determine burnup by analyzing γ-emitting nuclides inside the fuel elements. Activity measurements along the axis of an irradiated fuel element can be used to determine relative and absolute burnup. Through gamma spectroscopy, information about fuel composition and fission rates can be obtained by selecting appropriate gamma peaks and evaluating their ratios to determine their burnup.

The work of this thesis pursues another nondestructive technique called the "reactivity method" for generating new experimental data that can help identify the present composition and to verify the historical inventories of KSU TRIGA spent fuel. Therefore, preparations were made in support of this work to compile and assess the available data from the operation history of the KSU reactor. The reactivity method is an indirect method that relates reactivity worths to burnup and can be implemented using the positive-period method to measure the positive asymptotic period of an element. The period is the length of time required for the reactor power to increase by a factor of e$\approx$2.718. This quantity can be used in the inhour equation to determine reactivity. The work of this thesis also uses Serpent[6] and MCNP[7] models to determine axially-zoned fuel compositions and various kinetics parameters.

1.2 Background and Problem Description

The KSU TRIGA MARK II reactor first went critical in 1962 and has been actively used for research since. The KSU reactor had a license upgrade in 1968 and, as a result, the reactor fuel was replaced in 1973 with stainless steel (SS) clad fuel, much of which still remains in the core today. Since then, the reactor has had 29 different core configurations, i.e., different arrangements of fuel elements inside the core. New arrangements with shuffled positions or addition of fuel are necessary to compensate for reactivity loss over time. Typically, one additional element is added and another is shuffled when changing core configurations. When the KSU reactor received the license to increase up to 1250 kW in 2008, major shuffling of the core elements occurred such that inner core element were placed in the outer region of the core. Additionally, a new control was installed called the Safety Rod. The detailed power history of each configuration is thoroughly documented in the operational log books in addition to day-to-day documentation of water and fuel temperatures, control rod heights, and water conductivity. Currently available data includes operational log books and historical documents that date back to the first shipment of stainless steel cladding fuel to the KSU reactor. Documents of these initial shipments show that all but a few of the fuel elements received had burnups ranging from approximately 1 g to 11 g of the original ^{235}U content, with most elements having approximately 4 g to 6 g of burnup. Other fuel elements shipped in the latter years had an average burnup of approximately 0.7 g. Table 1.1 provides the assumed accumulated burnup for all the fuel elements received at KSU per shipment date.

Table 1.1: Accumulated burnup for all shipments of TRIGA fuel.

Shipment Date	Number of elements	Total Burnup (g of ^{235}U)
1973	88	350.9
1985	18	12.51
1995	4	0
1999	4	0
2005	4	0
2011*	6	0

*12% weight fuel awaiting NRC approval for use.

A detailed description of how these burnup values were estimated is provided in Chapter 2. All of these documents provide no information on burnup uncertainties and initial compositions, which make the recorded values hard to verify. Moreover, the depletion of these fuel elements in the KSU reactor further complicates the quantification of the burnup and, hence, composition.

The current methodology used by the KSU TRIGA staff to estimate fuel burnup also suffers from great uncertainties. The burnup of the unknown fuel elements is estimated by converting the core burnup from the log books for all the fuel element's length of time in the core to ^{235}U grams burned. A detailed description of core burnup calculations in (kWh) and uncertainty within the methodology is also discussed in Chapter 2. This estimation is admittedly inaccurate due to its approximations. One major approximation is assuming a uniform power distribution in the core by dividing the total core burnup equally among the core fuel. Another major approximation is assuming that all fissions born are a direct result of ^{235}U thermal neutron capture. Not only is this approximation confined to a specific energy, but it also assumes that all fissions are from one fissile isotope and thereby ignores fission in ^{238}U and isotopes of Pu produced during operation. These approximations lead to under- or over-predicting the fuel burnup.

There exists a lack of new benchmark data to help identify the composition of these fuel elements. The uncertainty in the initial burnup of fuel elements in addition to the depletion in the KSU core further increases the uncertainties in the fuel composition. New experimental data from reactivity measurements will be important for ongoing efforts to quantify the core composition. In order to have a well defined relationship between reactivity and burnup, and well defined uncertainties, a consistent method to estimate initial burnup of depleted fuel is required. The current methodology creates too great an uncertainty due to simple approximations.

1.3 Motivations

The primary motivation of this work is to provide new experimental benchmark data to produce a detailed model of the KSU reactor. The model will serve as a predictive tool capable of developing new reactor physics experiments at the KSU reactor by accurately modeling the physics inside the TRIGA reactor. Moreover, future researchers are provided with time dependent composition data for verifying application-specific depletion studies. Another motivation for this work is to provide the KSU TRIGA MARK II staff a precise method for determining the fuel burnup. The work proposed provides an alternative to the current methodology of estimating burnup, which suffers from great uncertainties. The resulting relationship between reactivity worths and burnup can be used to determine total burnups for fuels that cannot be measured directly perhaps due to excessive radioactivity like the in-core fuel elements currently residing in the KSU reactor.

1.4 Objectives

The primary goal of this work is to develop a well defined relationship between reactivity and burnup along with computational work in support of efforts to understand the KSU reactor fuel composition. The present work will employ available out-of-core elements for the reactivity method, and aims to provide data in support to understand this composition. This work uses the positive-period method to measure asymptotic period to solve for reactivity via the inhour equation. Reactivity measurements will indirectly determine the burnup of KSU TRIGA fuel elements with quantifiable uncertainty. The total burnup of the fuel is limited to element-integrated values; however, these can serve as measurable data points against which computed estimates can be benchmarked. Specifically, this work uses Serpent to estimate the compositions of burned fuel as an input in MCNP to extract the kinetics parameters needed as input to the inhour equation. The multiplication factor k_{eff} from MCNP is also used to calculate reactivity for modeling comparisons.

To support this goal, operational log history, current periodical burnup estimations performed at the KSU reactor, and documented fuel inventories for initial estimates of burnup are all addressed in Chapter 2. A review of the reactivity method and its previous application is provided in Chapter 3. The experimental procedure and the reactivity measurements performed at the KSU reactor by the means of positive period measurements are discussed in Chapter 4. MCNP6 and SERPENT results are described and summarized with the analysis of the experimental efforts in Chapter 5 followed by a conclusion in Chapter 6.

Chapter 2

Reactor Historical Data

This chapter aims to provide the reader with an overview of the history of KSU TRIGA fuel, the initial burnup inventories prior to KSU reactor use, and the available KSU operational log book data.

2.1 Fuel history

In 1973, the United States Atomic Energy Commission (AEC) approved the transfer of TRIGA fuel stainless steel (SS) clad elements, developed by General Atomics (GA), San Diego, California to KSU reactor. These TRIGA MARK III type fuel elements contain approximately 8.5 weight percent of uranium enriched to 20 percent in ^{235}U homogeneously combined with a zirconium hydride moderator with a hydrogen-to zirconium atom ratio of approximately 1.7 to 1. As shown in Figure 2.1, the fuel elements have an active region of approximately 15 inches long and 1.43 inches in diameter with a 0.18 in. diameter zirconium rod in the center to facilitate hydriding.

The fuel moderator elements have an inherent safety feature that allows a TRIGA reactor to return the reactor power to a normal level in the event of a power excursion, i.e., the fuel has a large prompt negative temperature coefficient of reactivity. Graphite end sections of the fuel elements serve as reflectors and are

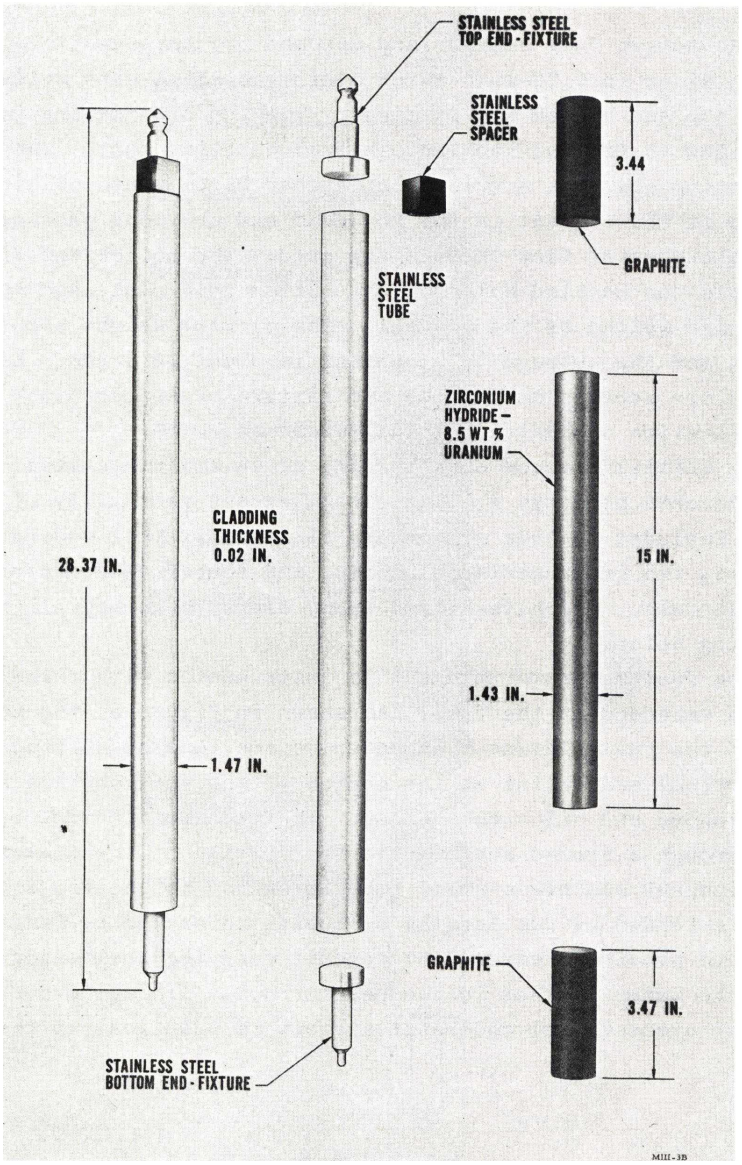

FIGURE 2.1: KSU reactor standard TRIGA fuel.[1]

approximately 3.47 inches long and 1.43 inches in diameter. The active fuel and graphite sections are contained in 0.02 inch thick stainless steel cladding welded to the top and bottom end fittings. The top end fitting is designed to fit and lock into a fuel handling tool and also has a triangular spacer block that positions the top of the element in the top grid plate. The bottom end fitting is designed to fit into sloping edge holes of the bottom grid plate for support of the entire weight of the element. These elements weigh approximately 3.4 kg, and the average ^{235}U

content before any depletion is about 38 g. Among these fuel elements, there are several instrumented elements which contain a thermocouple at three axial points within the fuel meat. These instrumented elements provide a watertight conduit carrying the wires above the water surface in the reactor pool for fuel temperature readings.

The fuel elements with stainless steel cladding (SS) were introduced to allow continued operation of the KSU reactor as the previous aluminum clad fuel became too weak for full-power operations. In 2008, when the reactor license was renewed, the maximum power level was upgraded to 1250 kW and a new control rod was installed. However, the current maximum power level is limited to approximately 660 kW based on the available fuel; KSU is waiting for NRC approval to use 12% uranium fuel, which will allow operation at 1 MW.

Between 1973 and 2016, there have been a total of 29 critical configurations of the KSU reactor with approximately 100 core fuel elements. The KSU reactor core consists of a concentric cylindrical lattice that is surrounded by a 12 in. thick graphite reflector enclosed in aluminum casting with a total of six rings: A, B, C, D, E, and F, having 1, 6, 12, 18, 24, and 30 locations, respectively. With the exception of components like control rods, graphite elements, a neutron source, and irradiation channels, the reactor core over the course of these configurations was occupied mostly by fuel elements. The changes in core configuration are due to addition of new fuel and the shuffling positions of in-core elements. Fuel elements closer to the center of the core experience a relatively high neutron flux and thus deplete faster. Therefore, when deemed necessary, the KSU reactor staff place those elements in the outer regions of the core. The KSU core lattice geometry is depicted in Figure 2.2.

A large portion of the fuel elements in the current configuration are from the initial loading of the SS fuel elements in 1973. The majority of these fuel elements had been depleted at the TRIGA MARK III reactor in GA laboratories, with an average burnup of just over 4 g of original ^{235}U content, when loaded. The rest of the fuel elements came from other fuel shipments in the latter years that were

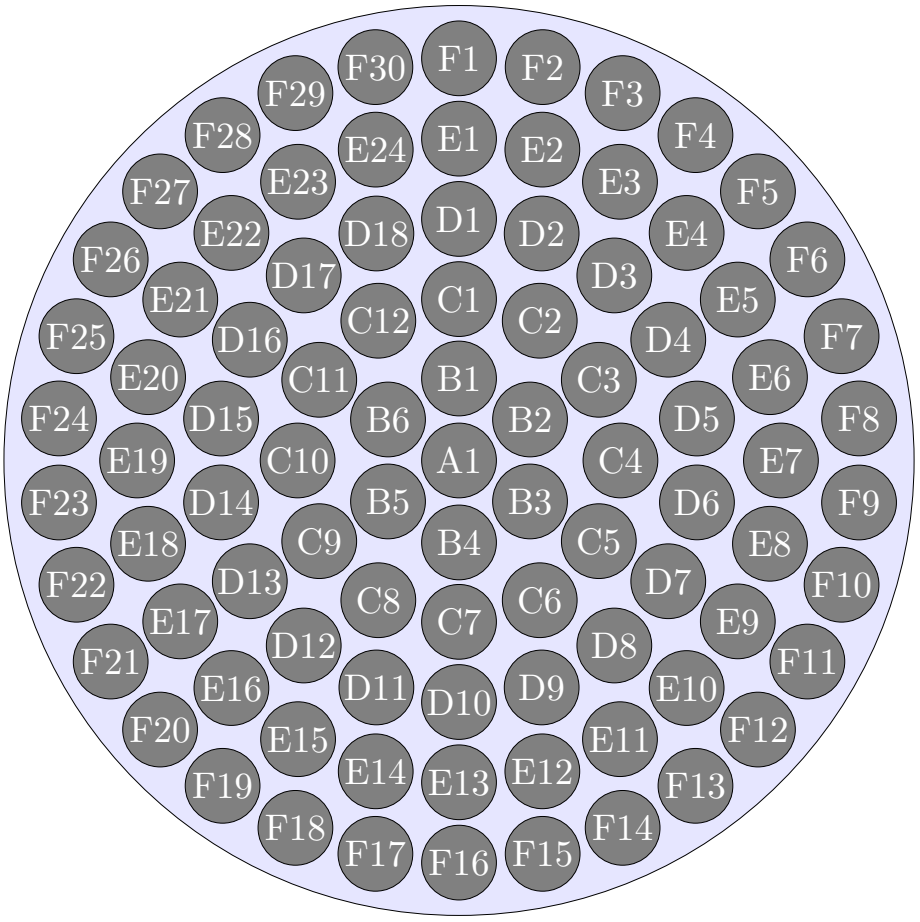

FIGURE 2.2: KSU reactor lattice geometry.

periodically added to the core when necessary to compensate for reactivity loss or to replace damaged fuel. Some of these elements came from a 1985 shipment from Northrop corporation following their decision to decommission their TRIGA F Reactor. These fuel elements had an average burnup of approximately 0.7 g. The remaining elements were fresh when loaded and came from a 1995 shipment from GA and 1999 and 2005 shipments from CERCA (Compagnie pour l'Étude et la Réalisation de Combustibles Atomiques).

Knowledge of the burnup of the initial loading of elements is essential to determine the present composition of the KSU TRIGA reactor. More importantly, for the purposes of this work, the study of out-of-core elements relied heavily on the reported burnup along with known depletion received at the KSU reactor. Fortunately, among the associated fuel documents available at KSU, a report describes the method previous TRIGA reactor facilities used to calculate the burnup

in g of ^{235}U during its time in their facility. These initial burnup calculations along with the current burnup from the operational log books at the KSU reactor can be used to provide the overall burnup of the fuel elements of interest.

2.2 Initial burnup of KSU TRIGA fuel

The burnup of these initial fuel elements consumed substantial ^{235}U content prior to installation at KSU. The previous TRIGA facility at GA used a standard report that dates back to 1969 that outlined the method to calculate the burnup of ^{235}U in TRIGA fuel. Eq. (2.1) defines the amount of ^{235}U consumed of an individual element,

$$G_j = 1.24 \sum_i \frac{P_i E_i}{N_i} \tag{2.1}$$

where G_j is the amount of ^{235}U consumed in the jth element in grams, P$_i$ is the ratio of the ring average power density in the ith fuel position to the average in the core, E$_i$ is the integrated reactor energy generated while the jth element was in the ith position in MWD, and N$_i$ is the number of elements in the core during the time that the jth element was in the ith position. For a typical 250 kW TRIGA reactor operating 200 days a year and 8 hours per day, the ^{235}U consumption is approximately 20 g per year[8]. Thus, the rate of consumption is about 1.24 g of ^{235}U per MWD of thermal power production, as used in Eq. (2.1). A standard calculation for the consumption and conversion of thermal power production to ^{235}U grams burned is provided in Appendix A.

Enclosed in the same report was a burnup summary card of one of the fuel elements initially burned at the TRIGA MARK III reactor in San Diego before its transfer to KSU. Like the KSU TRIGA reactor, the TRIGA MARK III reactor had circular rings but included an additional outer G ring. The power peaking factors for the rings were also included in the report (see Table 2.1). As seen in Table 2.2, the summary card indicates the in-core history of fuel element 3113. For simplicity, it

TABLE 2.1: Specified Ring Power peaking factor.

Ring Position	P_i
A	1.61
B	1.57
C	1.46
D	1.29
E	1.07
F	0.81
G	0.66

was assumed that there were 120 fuel elements, i.e., N_i=120, in the core during the lifetime of fuel element number 3113.

TABLE 2.2: Burnup summary card for Fuel element 3113 prior to KSU depletion.

Ring position	Length of time	MWD	Number of elements in core
C	08/04/1964-01/28/1965	107.44	120
E	01/28/1965-06/10/1971	161.07	120

The total amount of U^{235} consumed is, then,

$$G_{3113} = 1.24 \sum_i \frac{1.46 \times 107.44 + 1.07 \times 161.07}{120} = 3.29\,\text{g}. \tag{2.2}$$

Further information on the integrated reactor power in MWD from the facility's operational data or how the power peaking factors and related uncertainties were calculated were not documented. For the purposes of maintaining consistency, the preliminary burnup calculations of tested fuel elements for the reactivity method in this work were calculated using Eq. (2.1). The KSU core ring power peaking factors used in the calculations for further accuracy are discussed in Chapter 5.

2.3 KSU Logbook data

The KSU operating logbooks contain records of the power history since the reactor first went critical in 1962. These records consist of all operations and events

which affect the reactor, including changes in reactor configuration, fuel loading, control rod position and worth, and insertion of experimental apparatus. In a day of operation, reactivity manipulations such as startup, shutdown, and power changes are recorded by the reactor operator on duty. Logbook entries, as shown in Figure 2.3, for each operating day take the following form: time of event; person reporting; power level channel readings; control rod positions; fuel and water temperature readings; description of event.

Date:		Core:			Checklist Page #:					Continuation Page:				Supervisor Signature:					
Time	Operations Information				Operating Data														Status
					Power	Control Rod Position				Power Level Readings				Cooling Temp			Fuel Temp		
	Run	Operator	Supervisor	Trainee		Pulse	Safety	Shim	Reg	NLW	NMP Range	NMP % Range	NPP % Power	Inlet	Outlet	Bulk	#1	#2	

FIGURE 2.3: log sheet.

Startup procedures begin by entering the reactor conditions as indicated by the instrumental readings before any control rod movements. Afterwards, control rods are then used one at a time for a desired power level. Since 1962, these logbook entries have changed in structure but maintained time entries for power levels during power changes with a maximum of a five minute delay in recording according to the operational limitations[9]. Reactor operators will thus wait to enter the time in critical sets, i.e, when $k_{\text{eff}} = 1$, until power stabilizes. Finally, the time entry for the shutdown of the reactor is recorded following the insertion of the control rods.

There are three indications of power that operators record in the logbook. First, the NLW (Nuclear Logarithmic Wide Range) power channel, which uses a fission

counter for detecting thermal neutrons incorporating pulse height discrimination to distinguish neutron pulses from gamma pulses at low power levels. Second, the NMP (Nuclear Multi-Range Power) channel uses a compensated ion chamber for detection of thermal neutrons, which provides a multi-range linear power indication. The NPP (Nuclear Percent Power) channel, coupled to an uncompensated ion chamber, provides power reading percentages of 1 MW. Incremented burnup generation is reported each day of operation and are added to the overall burnup generation since the reactor first went critical. Estimates of burnup generations in kWh are calculated using the rectangle method of integration over the power dependent time data in critical log sets and shutdown periods and neglect any startup power generation. Critical log sets are reported using the NMP channel as the main indication of power. These estimations were designed such that neglected startup power generation would be compensated by overestimating the shutdown periods.

TABLE 2.3: The discrete steps for a simple operational day.

Time	Power (kW)	status
01:28:00 PM	0	startup
01:35:00 PM	0.01	$k_{\text{eff}} = 1$
01:38:00 PM	0	shutdown
03:08:00 PM	0	startup
03:19:00 PM	200	$k_{\text{eff}} = 1$
03:51:00 PM	500	$k_{\text{eff}} = 1$
04:51:00 PM	100	$k_{\text{eff}} = 1$
05:00:00 PM	0	shutdown

To illustrate these estimations, Table 2.3 summarizes a simple day of operation where discrete steps such as startups, critical operation, and shutdowns are included. Figure 2.4 depicts the power data from the NLW and NMP power channels and illustrates the rectangle method of integration by approximating the definite integral, highlighted in blue rectangles. There was not a recording of power from the NPP channel in the stripchart recorder on that day. Based on the method used by the reactor staff, the total power generation would be 621.67 kWh or 0.026 MWD. As observed in Figure 2.4, the method underestimates during startup power levels but overestimates the power generation during shutdown. Since 2011 the KSU reactor

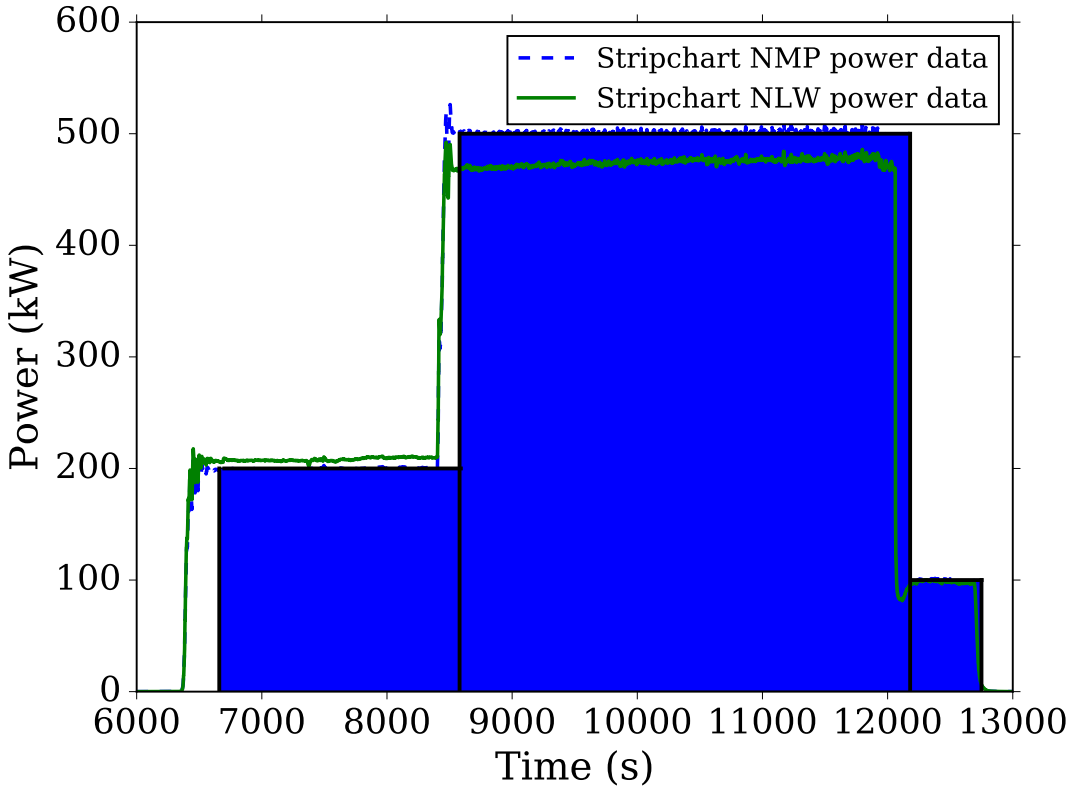

FIGURE 2.4: Power data with mock up estimations burnup.

facility used an SV 180 digitized strip-chart recorder, a paperless data acquisition system, that records power level readings and fuel and water temperatures every second. For the same day of operation in the example above, the total power generation according to the NLW and NMP channels is 610.67 kWh or 0.025 and 632.43 kWh or 0.026 MWD, respectively. The digitized recording can be used to calculate a more accurate power generation by integration of the time dependent power data. Moreover, the transition to recording power generations per second from the stripchart recorder could help quantify the uncertainties in the burnup calculation. For the purposes of this work, only uncertainties introduced later from the power factor calculations were determined, see Section 5.3.

Chapter 3

Literature Review

This chapter describes the relationship between reactivity and burnup, and how that relationship is used via the "reactivity method" to determine fuel burnup. Past use of the reactivity method and its sensitivity to isotopic uncertainties is also summarized.

3.1 The Reactivity Method

The reactivity method is an indirect technique for estimating burnup (and, therefore, composition) based on the assumption that the reactivity worth of a fuel element is a known function of burnup. In this method, fuel elements of interest are placed in a specific "measurement" location within a core configuration established to be approximately supercritical (reactivity $\rho > 0$) with all control rods fully withdrawn before an element is inserted. The positive period method is among a variety of experimental techniques that have been developed to measure fuel reactivity worth and was chosen for this work due to its simplicity. With this technique, reactor periods are determined by analyzing the power transient resulting from the reactivity insertion and later used in the inhour equation to determine the reactivity. The core excess reactivity, i.e., the reactivity remaining when the control rods fully withdrawn, is the only measured quantity needed to determine a fuel

element's reactivity worth. The respective reactivity worth is equal to the difference of core excess reactivity before and after insertion of a fuel element. The core configuration used for this work and the procedure for the positive period method are addressed in Chapter 4.

Reactivity is a parameter that indicates a nuclear reactor's departure from criticality, i.e., when the k_{eff} of the system is 1 and a reactor is sustaining a fission chain reaction, defined in Eq. (3.1). The effective multiplication factor k_{eff} can be defined as the ratio of the neutrons produced in a reactor in one generation to the number of neutrons produced in the previous generation;

$$\rho = \frac{\Delta k_{\text{eff}}}{k_{\text{eff}}} = \frac{k_{\text{eff}} - 1}{k_{\text{eff}}}, \tag{3.1}$$

where the reactor state, with a given value of k_{eff}, is defined as

$$\begin{aligned} k_{\text{eff}} &> 1 \quad \text{supercritical} \\ k_{\text{eff}} &= 1 \qquad\quad \text{critical} \\ k_{\text{eff}} &< 1 \quad \text{subcritical.} \end{aligned} \tag{3.2}$$

Generally, the reactivity worth of a fuel element decreases with increased burnup, and often a simple relationship between burnup and reactivity can be established. In particular, if at least two of the measured fuel elements have well-specified burnups, a linear relationship between reactivity and burnup can be defined. This relationship can be used to determine total burnups for fuel elements that cannot be measured directly (due, perhaps, to excess radioactivity). It is convenient to use a fresh element, i.e., no burnup, to serve as a lower bound in the defined relationship. Nonetheless, if a fresh element is not available, two or more elements can be picked for references as long as its burnup is determined with sufficient accuracy. Therefore, it must be emphasized that the reactivity method is a relative method and another method, such as gamma spectroscopy or reactor physics calculations, must be used for a supplementary absolute burnup determination if an additional reference

point is needed. For the purposes of this work, the reactivity method was used as the primary technique to define a relationship between reactivity worths and burnup along with support from computational modeling; additional supporting measurements via gamma spectroscopy are planned at KSU.

3.2 Summary of Past Work

The relationship between reactivity and burnup depends significantly on the fuel in question. The accuracy of calculated burnup varies significantly from element to element and if one type of fuel has been used in regions with another type. Previous applications of the reactivity method had to account for such effects because many TRIGA facilities operate with mixed fuel types. At the KSU reactor, only one type of fuel has been used for the operational history considered, however, it is not clear whether much of the spent fuel had been depleted where operations had mixed fuel types[10]. This section aims to provide a summary of past applications of the reactivity method and the significance of fuel elements that spent most of their core lifetime around heterogeneities that cause irregular flux distributions.

3.2.1 Initial Work

The reactivity method was first introduced in early work performed at the Atominstitut TRIGA MARK II reactor to provide an alternative method for determining fuel element burnups based on the measurement of the element's relative reactivity worth[2]. The facility operated with mixed fuel that included stainless steel (SS) and aluminum (Al) cladding both with 8.5 weight (wt) % uranium enriched to 20% in ^{235}U and FLIP (Fuel Lifetime Improvement Program) fuel that was 8.5wt % in uranium and 70% enriched in ^{235}U. The reactivity measurements were performed only with in-core Al and SS clad fuel elements. In-core FLIP fuel were not experimented with since they were necessary to compensate the reactivity loss during the vacancy of the tested fuel elements. A measurement location was chosen in

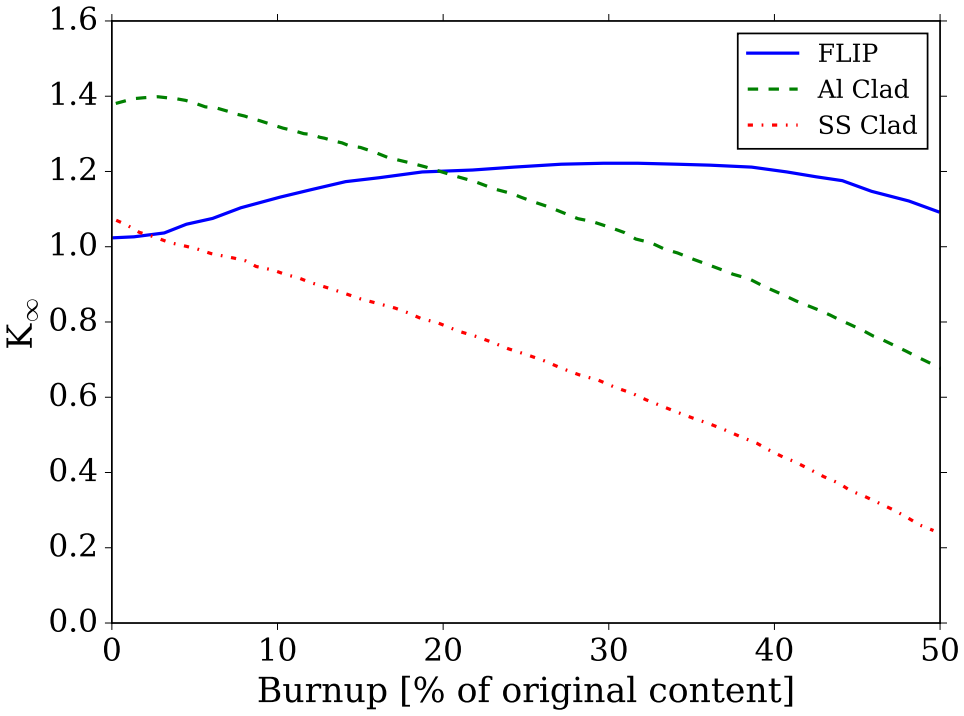

FIGURE 3.1: K_∞ versus % burnup for Al, SS, and FLIP fuel after ref.[2].

the C-ring, an inner ring, though the reason for choosing this location was not specified. Prior to the reactivity measurements, the dependence of reactivity on burnup for all the TRIGA fuel element types in the reactor were tabulated using the TRIGAP computer code, a one-dimensional, two-group diffusion approximation code in which group constants were calculated using the WIMS code[2][11][12]. The calculation was done to understand the dependence on burnup of those fuel types and to give insight into how these correlations could affect the reactivity measurements, especially for elements used in mixed-fuel configurations.

As shown Figure 3.1, the multiplication factor (or reactivity) of low enriched uranium (LEU) fuel exhibits a linear dependence on burnup while that high of enriched uranium (HEU) fuel has a strong non-linear dependence on burnup. Non-linearity in burnup is observed for the case of Al cladding at lower burnup and FLIP fuels because of burnable poisons, samarium and erbium, included in the fuel elements[2]. It is important to note, as mentioned in Section 2.1, that the KSU TRIGA fuel had SS cladding with no burnable poison. However, samarium is a

fission product that builds up over time, and several of its isotopes are important to include in burnup calculations.

The reactivity measurements were conducted by observing the variation in the neutron flux signal by a digital reactivity meter. This meter has a range -20 to +300 pcm ("per cent mille" equals 10^{-5} $\frac{\Delta k}{k}$)), which allowed measurements at subcritical conditions to be taken into account[2]. The reactivity measurements were performed along with the predictive TRIGAP code for both types of fuel to compare the experimental to reactor calculational techniques in estimating the burnups of the measured fuel elements. It was concluded that the differences were due to the simplifications of the TRIGAP models that inadequately treated the irregularities of flux distributions caused by the mixed fuel. FLIP fuel has a thermal absorption cross section of approximately seven times that of standard fuel[13]. This led to large variations in the final burnup calculations of the reactivity measurements that were performed. Furthermore, some of these measured fuel elements were near graphite reflector elements, control rods, and water-filled assemblies during their lifetime in the core, and the model inadequately treated these irregularities. There was no specific uncertainty analysis in the reactivity results in this early work, and therefore, benchmark experiments conducted at the Josef Stefan TRIGA MARK II reactor in Ljubljana, Slovenija were reviewed.

3.2.2 Reactivity measurements at Josef Stein TRIGA reactor

At the Jozef Stefan TRIGA reactor in Ljubljana, Slovenia, two benchmark experiments were performed in which several parameters (multiplication factor, fuel temperature reactivity coefficient, fuel element reactivity worth distribution, radial and axial flux distributions, among others) were measured in 1991 and again in 1998. These benchmark experiments were conducted to test computer codes for research reactor fuel management and burnup calculations. Since reconstruction began in 1990, the reactor has operated with only standard SS clad 20% enriched TRIGA fuel that included used 8.5wt % and new fresh 12wt % fuel. Specifically, in the

second benchmark experiment, fuel element burnup was measured by the reactivity method in which the measurements were performed in an experimental core configuration loaded only with 12wt %, 20% fuel. This configuration was constant during the experiments since the measurements were relative. The measurement location was chosen in the C-ring, near the center of the core. It was chosen because the fission rate was high, and the gradient of neutron flux was approximately constant. The control rods were fully withdrawn during the reactivity measurement, and a reactivity meter, similar to that at the Atominstitut reactor, was available to analyze the flux time dependent data to measure reactivity.

A total of nine standard 12wt % 20% enriched TRIGA fuel elements were selected for measurements. It is important to note that three of them had spent most of their core lives near control rods and irradiation channels and one in a mixed ring with 8.5 wt % 20 % enriched fuel. The rest of these elements had relatively simple burnup histories, and one, included approximately fresh element, which served as a reference element for absolute burnup determination[3].

The first set of reactivity measurements were performed only 20 hours after the reactor had been operating at full power (250 kW). The total thermal energy produced from that operation, approximately 6.4 MWh, led to high xenon (Xe) presence in the reactivity measurements. One measurement was observed to have a difference of approximately 7 pcm in a 132 minute interval. For that reason, all the measurements were repeated after 40 hours after shutdown to eliminate the Xe influence. Subsequently, reproducibility of the same reactivity measurement had shown a ± 1 pcm difference in a 97 minute interval. Since some of the elements had spent their core lives under irregular flux distributions, the orientation of two fuel elements were studied by rotating them around their axis and observing the difference in the reactivity measurement. Measurements of the elements showed that the effect contributes about ± 8 pcm[3].

The results of these measurements were compared to modeled reactivity worths from TRIGLAV, as shown in Figure 3.2[14]. TRIGLAV is based on a four-group, two-dimensional theory model in which every location in a given core configuration

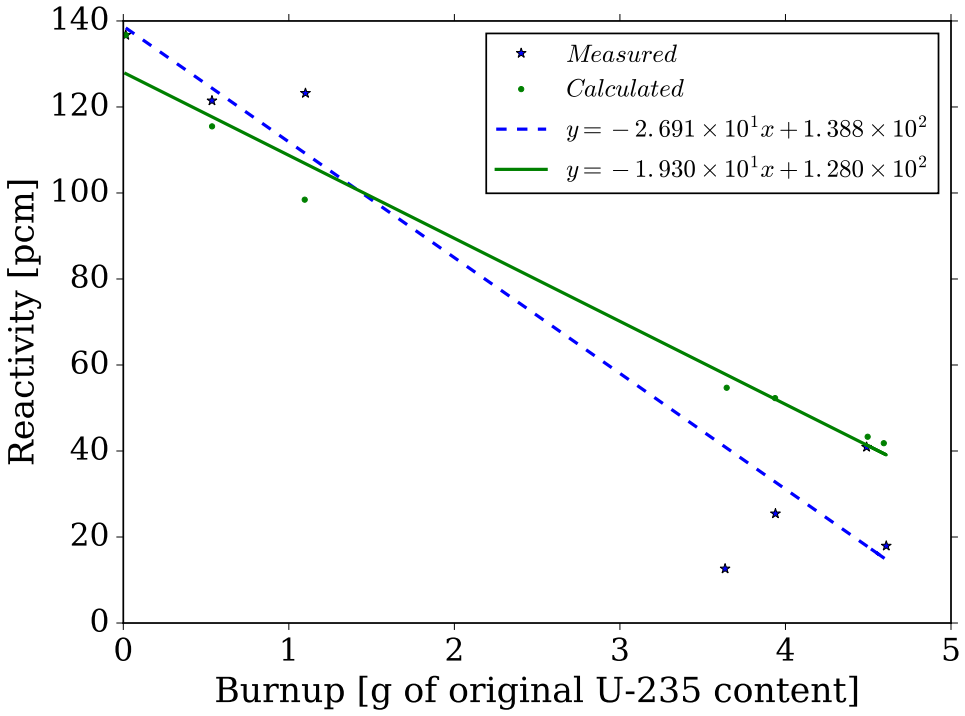

FIGURE 3.2: Reactivity versus burnup for Josef Stefan TRIGA fuel after.[3]

is treated explicitly as a homogeneous region equivalent to a unit cell. TRIGLAV was shown to be a good predictor of burnup for almost all of the fuel elements and showed good agreement within ±1% burnup. One element showed that the burnup calculation was too low due to the uncertainty in initial hydrogen and zirconium content which contributed to a reactivity change of approximately 30 pcm and was equivalent to the reactivity loss due to a burnup of 1.5 MWd/MTU.

3.2.3 Sensitivity studies of burnup composition

Sensitivity studies of the TRIGA benchmark critical experiment were performed to estimate the effects of various uncertainties on the effective multiplication factor using reactor calculation codes to validate the experimental results. Most notably, the effects of fuel composition were investigated to observe the effects it would have on k_{eff} modeled calculations. Between the two benchmark experiments, the fuel element burnup accumulated during 1991-1998 was calculated with TRIGLAV. The isotopic compositions for these elements were supplied to TRIGLAV using WIMD4

code for each fuel element at a particular burnup. In an aim to conduct these sensitivity studies on compositions, a Monte Carlo model that was developed in 1997[15] was used to observe the effect of the inclusion and exclusion of several isotopes at different burnups. To extend that analysis, WIMSD4 results were compared to ORIGEN2 results for fuel isotopic composition importance. Calculations of the standard TRIGA fuel element isotopic composition as a function of burnup were performed for 3%, 10%, and 20% burnup of ^{235}U. It was concluded that only ^{135}Xe, ^{149}Sm, ^{151}Sm, ^{239}Pu, and ^{143}Nd are important for criticality calculations if burnups are less than 5%. For higher burnups (burnup $>$ 10%) an additional 7 isotopes (^{236}U, ^{147}Pm, ^{103}Rh, ^{131}Xe, ^{133}Cs, ^{99}Tc, and ^{240}Pu) had to be included yeilding a $\pm$ 10% uncertainty in the change of k_{eff} due to burnup. It also was concluded that both WIMSD4 and ORIGEN2 gave similar burned material compositions and the differences observed in some isotope concentrations had very little impact on the criticality calculations.[16] The isotopes included in the computation efforts for this work are discussed in more detail in Chapter 5.

Chapter 4

Experimental Procedure

To calculate the reactivity worth of a fuel element via the positive period method, the inhour equation is required, the theory of which is given first. The experimental procedure for the measurements at the KSU reactor is then described followed by a brief overview of the experimental data output from the stripchart recorder.

4.1 Theory

The theoretical relationship between the stable or asymptotic period of a reactor and the corresponding reactivity responsible for that period is developed in this section. The time-dependent behavior of a reactor is related to the effective multiplication factor and its deviation from criticality. The power produced during a reactor transient is not only related to k_{eff} but also to the prompt and delayed neutron properties through the reactor kinetics equations as will be shown later. Fission is a process in which the nucleus of a heavy atom splits into lighter nuclei, simultaneously ejecting free neutrons and releasing large amounts of energy. More than 99 percent of fission neutrons produced are prompt neutrons. They are born instantaneously at the time of fission and have a lifetime, i.e., the length of time at which a neutron is born until its absorption by surrounding medium or escaped from the system, of 10^{-5} to 10^{-4} seconds[4]. The prompt neutron lifetime is dominated

by the slowing down time to thermal energies and its subsequent diffusion time before being removed from the system. With these small neutron lifetimes, it is difficult to manage the rates of change in neutron populations even for a small step change of reactivity. However, the remaining fraction, known as the delayed neutron fraction, has a great impact in decreasing the rate of change in the neutron population. Delayed neutrons are the result of the decay of neutron-emitting fission products. They are typically lumped in the framework of groups, known as neutron precursors, based on their half-lives; see Table 4.1 for typical delayed neutron properties for ^{233}U, ^{235}U, and ^{239}Pu. Half lives, i.e., the time taken for one-half of the atoms of a radioactive isotope to undergo radioactive decay, of these precursors range from a fraction of a second to nearly a minute, and they dominate the average neutron lifetime making it possible to manage the rates of change in the neutron population. As seen in Table 4.1, the delayed neutron precursors are divided into 6 groups, and the new features from MCNP also provide the same number of groups.

TABLE 4.1: Delayed Neutron properties.[4]

Group	Approximate Half Life(sec)	Delayed Neutron Fraction		
		^{233}U	^{235}U	^{239}Pu
1	56	$2.3 \cdot 10^{-4}$	$2.1 \cdot 10^{-4}$	$0.7 \cdot 10^{-4}$
2	23	$7.8 \cdot 10^{-4}$	$14.2 \cdot 10^{-4}$	$6.3 \cdot 10^{-4}$
3	6.2	$6.4 \cdot 10^{-4}$	$12.8 \cdot 10^{-4}$	$4.4 \cdot 10^{-4}$
4	2.3	$7.4 \cdot 10^{-4}$	$25.7 \cdot 10^{-4}$	$6.9 \cdot 10^{-4}$
5	0.6	$1.4 \cdot 10^{-4}$	$7.5 \cdot 10^{-4}$	$1.8 \cdot 10^{-4}$
6	0.2	$0.8 \cdot 10^{-4}$	$2.7 \cdot 10^{-4}$	$0.9 \cdot 10^{-4}$

The point reactor kinetics equations (PRKEs) are an approximate model of the time-dependent reactor behavior. From this model, the inhour equation is derived to determine reactivity through a relatively simple period measurement. In the PRKEs model, the reactor power varies proportionally throughout its volume, considering only an average value of the power density. The PRKEs uses the one-speed approximation in which the neutron distribution and the associated cross sections are averaged over energy. Moreover, an assumed time-independent spatial flux shape is approximated by a non-leakage probability which removes

the need to treat spatial effects. These approximations are defined primarily to emphasize the study of time dependent behavior of a nuclear reactor.

The derivation of the PRKEs begins by introducing the neutron balance equation for a finite reactor. For simplicity, we consider only neutrons, of one speed:

$$\begin{aligned} \frac{dn(t)}{dt} &= \text{source neutrons produced} + \text{fission neutrons produced} \\ &\quad - \text{neutrons absorbed} - \text{neutrons leaked from the system} \\ \frac{dn(t)}{dt} &= S(t) + \bar{\nu}\Sigma_f \bar{v} n(t) - \Sigma_a \bar{v} n(t) + D\nabla^2 \bar{v} n(t) \end{aligned} \tag{4.1}$$

where $S(t)$ is the strength of the external neutron source in the reactor, $n(t)$ is the neutron density, $\bar{v}$ is average neutron speed, Σ_a is the energy-averaged cross section for absorption, Σ_f is the energy-averaged cross section for fission, $\bar{\nu}$ is the average number of neutrons produced per fission, and D is the diffusion coefficient.

For a steady-state, critical reactor for which $\frac{dn(t)}{dt} = 0$, Eq. (4.1) simplifies to,

$$\bar{\nu}\Sigma_f \bar{v} n(t) - \Sigma_a \bar{v} n(t) + D\nabla^2 \bar{v} n(t) = 0. \tag{4.2}$$

Notice that the extraneous source is omitted from Eq. (4.2). This is because in a critical state, the production term is independent of any extraneous source and dependent only upon fission neutrons from the fuel, assuming $\bar{\nu}\Sigma_f \bar{v} n(t) >> S(t)$. The quantity L, called the diffusion length, can be defined by $L^2 = \frac{D}{\Sigma_a}$. Here L quantifies the distance a neutron travels to absorption. Furthermore, the quantity k_∞, taken here as the infinite multiplication factor, can then be defined as $k_\infty = \frac{\bar{\nu}\Sigma_f}{\Sigma_a}$. Substitution of L and k_∞ into Eq. (4.2) simplifies to the following equation:

$$\nabla^2 \bar{v} n(t) - \frac{k_\infty - 1}{L^2} \bar{v} n(t) = 0. \tag{4.3}$$

By defining a quantity called "buckling", B^2, Eq. (4.3) then simplifies to

$$\nabla^2 \bar{v}n(t) - B^2 \bar{v}n(t) = 0. \tag{4.4}$$

The eigenvalue B^2 in the wave equation above can be expressed as the material buckling where the buckling is dependent on reactor materials, i.e., $B_m^2 = \frac{k_\infty - 1}{L^2}$. Additionally, B^2 dependence could also be expressed based on the geometry, i.e., the size and shape, of the reactor, where geometric buckling B_g^2 is a a measure of the bending or curvature of the neutron flux at any point (x, y, z) within the reactor,

$$B_g^2 = \frac{-\nabla^2 \bar{v}n(x, y, z)}{\bar{v}n(x, y, z)} = 0. \tag{4.5}$$

Notice the relationship of buckling to the leakage expression $D\nabla^2 \bar{v}n(t)$. A greater curvature of the neutron flux indicates a greater leakage from the reactor. Note that at a critical condition, $\frac{d\bar{v}n}{dt} = 0$ and $B_g^2 = B_m^2$, which can be used to give the critical dimensions of the reactor. Recall in Eq. (4.1) that the neutron leakage term is $D\nabla^2 \bar{v}n(t)$ and the absorption term is $\Sigma_a \bar{v}n(t)$. The thermal non-leakage probability can be defined as P_{NL}, i.e., the ratio of thermal absorption to the total loss of thermal neutrons, or the portion that did not leak from the system, where $D\nabla^2 \bar{v}n(t)$ is equal to $DB^2 \bar{v}n(t)$ (from Eq. (4.4)),

$$\begin{aligned} P_{NL} &= \frac{\text{Thermal absorption}}{\text{Thermal absorption} + \text{Thermal leakage}} \\ P_{NL} &= \frac{\Sigma_a \bar{v}n(t)}{\Sigma_a \bar{v}n(t) + D\nabla^2 \bar{v}n(t)} = \frac{1}{1 + L^2 B^2}. \end{aligned} \tag{4.6}$$

Eq. (4.1) then is reduced to

$$\frac{dn(t)}{dt} = S(t) + \frac{k_{eff} - 1}{l} n(t), \tag{4.7}$$

where

$$k_{\text{eff}} = \frac{\nu\Sigma_f}{\Sigma_a} P_{NL}$$
$$l = \frac{1}{\bar{v}\Sigma_a} P_{NL}. \tag{4.8}$$

Here, l is defined as the neutron lifetime and k_{eff} is the multiplication factor with leakage effects included. In reality, the total non-leakage probability also includes the non-leakage probability for fast neutrons when they are born from fission using the Fermi slowing-down theory. However, for the purposes of one-group calculations as indicated above, the non-leakage probability is well described in Eq. (4.6).

From Eq. (4.7) , we solve for the neutron population without extraneous sources of neutrons,

$$n(t) = n(0)exp\left(\frac{k_{eff} - 1}{l} t\right) \tag{4.9}$$

Recall that the period T is the time where the flux or neutron population to increase by a factor of e. Eq. (4.8) then becomes

$$n(t) = n(0)exp\left(\frac{t}{T}\right) \tag{4.10}$$

where the period is

$$T = \frac{l}{k_{eff} - 1}. \tag{4.11}$$

According to Eq. (4.10), for a change in k_{eff} from 1, i.e., steady-state critical reactor, to k_{eff}=1.001, and a thermal neutron lifetime of $4.3 \cdot 10^{-5}$, taken from KSU Safety Analysis Report, the period is 0.043 s. This would mean that in 1 s, the flux would rise by $\approx e^{23}$. The reactor would be completely out of control if this were

reality. Fortunately, the effect of delayed neutrons, which have been ignored until now, greatly decreases the rates of change in the neutron populations. Recall that delayed neutrons are well described in groups known as precursors. Rewriting Eq. (4.1), the neutron balance in which the effects of delayed neutrons are included takes the following form,

$$\frac{dn(t)}{dt} = S(t) + (1-\beta)\bar{\nu}\Sigma_f\bar{v}n(t) + \sum_i \lambda_i C_i(t) - \Sigma_a\bar{v}n(t) + D\nabla^2\bar{v}n(t) \qquad (4.12)$$

where β_i is the delayed fraction of the i-th group of delayed neutrons, C_i is the concentration of radioactive precursors produced of the i-th group, and λ_i is the decay constant of the delayed neutron precursors of the i-th group so that the rate of delayed neutron production is $\sum_i \lambda_i C_i(t)$.

In order to solve Eq. (4.12), it is important to determine the precursor concentration for each delayed group. This can be done with the following equation:

$$\begin{aligned} \frac{dC_i(t)}{dt} &= \text{Number of precursors produced/s} \quad + \\ &\qquad \text{Number of precursors decaying/s} \\ \frac{dC_i(t)}{dt} &= \beta_i\nu\Sigma_f\bar{v}n(t) - \lambda_i C_i(t). \quad i = 1, 2, ... \end{aligned} \qquad (4.13)$$

By using the definition of reactivity in Eq. (3.2) and designating the quantity $\frac{l}{k_{eff}}$ as Λ, Eqs. (4.12)–(4.13) can be reduced to the following linear ordinary differential equations that describe the time-dependent behavior of a reactor,

$$\frac{dn(t)}{dt} = S(t) + \frac{\rho-\beta}{\Lambda} + \sum_i \lambda_i C_i(t) \quad i = 1, 2, ... \qquad (4.14)$$

$$\frac{dC_i(t)}{dt} = \frac{\beta_i}{\Lambda}n(t) - \lambda_i C_i(t) \quad i = 1, 2, ... \qquad (4.15)$$

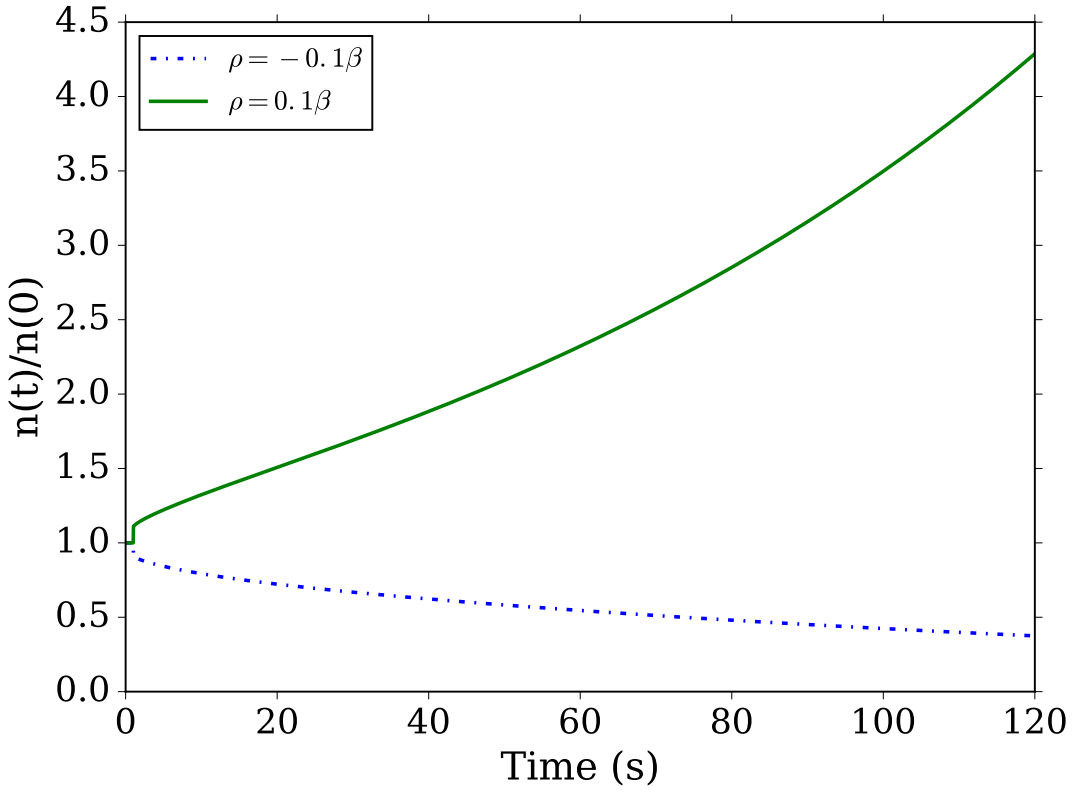

FIGURE 4.1: Reactivity Insertions of $\pm$ 0.10β at an initial critical reactor[4].

A Python script was written to illustrate the neutron population as a function of time using the point reactor kinetics equations and the KSU TRIGA delayed neutron data[9]. Fig. 4.1 depicts the time dependent behavior of the reactor power after a sudden positive as well as a negative change in reactivity in an initially critical reactor. For times less than one second, the prompt neutrons are abruptly in control of the neutron population. This is known as the prompt jump. The slow growth and decline of the two curves following the prompt jump occur because small reactivity insertions, $\rho < \beta$, cause the delayed neutrons to be the primary determinant of the neutron population. Subsequently, for large positive insertions of reactivity, $\rho > \beta$, it is apparent that the prompt neutron lifetime is the primary determinant of the reactor response. Modern units of reactivities are expressed in pcm or in dollars, where \$ =ρ/β. As ρ approaches β, the reactor period becomes shorter, making the reactor difficult to control. Avoiding such an approach is why units of reactivities are expressed in dollars[4]. Moreover, the asymptotic behavior of the neutron population is expressed in an exponential form, n(t) $\propto$ exp(t/T),

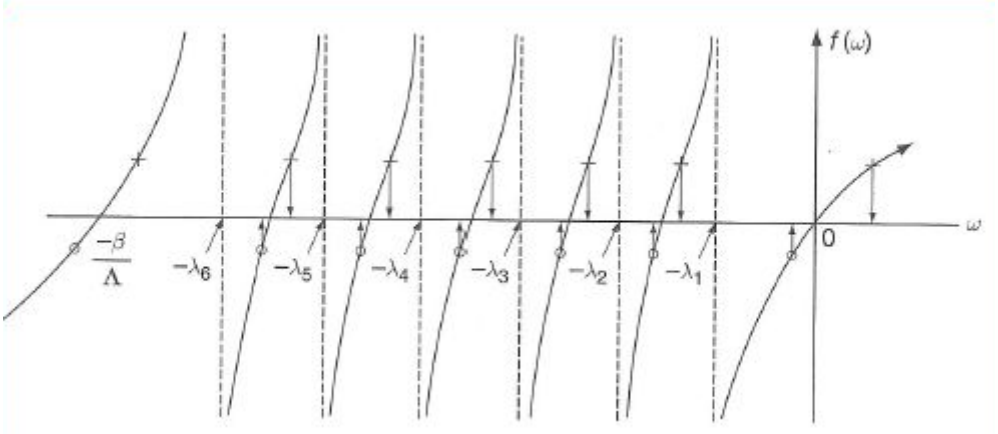

FIGURE 4.2: Solutions of the inhour equation[4].

where T is the asymptotic or stable period. Depending on whether the reactor is subcritical or supercritical, the reactor period is negative or positive, respectively.

To determine the reactor stable period, a well known equation in reactor theory, known as the inhour equation, is used to to relate the measured positive period to a positive step change in reactivity. This key equation is derived from the PRKE, where the solution of the ordinary differential equations of 4.16 and 4.17 are sought in the form of n(t)= N exp(ωt) and $C_i(t) = B_i\exp(\omega t)$, where N, B_i, and ω are constants. By substituting these forms in the kinetics equations, the solution yields

$$\rho = \mathrm{f}(\omega) = \omega\left(\Lambda + \sum_i \frac{\beta_i}{\omega + \lambda_i}\right), \tag{4.16}$$

where ρ is reactivity and ω is the inverse stable period.

Figure 4.2 depicts the graphical solution of Eq. (4.16) where i=6 for 6 precursor groups. Subsequently, there are a total of 7 eigenvalues, ω_i, for the solution of the inhour equation. Accordingly, the solution of the neutron density n(t) is expressed as a linear combination of the seven solutions,

$$\sum_{i=1}^{7} = N_i\exp(\omega_i t). \tag{4.17}$$

It is evident that for positive reactivities, only one root is positive, ω_1, and the rest are negative, which makes the remaining terms in Eq. (4.17) die away with time.

Negative reactivities show that all roots are negative, with ω_1 dying away more slowly than the other roots. Consequently, the asymptotic solution of the neutron population is,

$$n(t) \approx N_1 \exp(t/T) \tag{4.18}$$

where T = $1/\omega_1$ is the reactor stable period.

Note that a limiting period , i.e. T= $1/\lambda_1$ of the longest-lived group, is in place for negative changes in reactivity, which implies that a reactor cannot shutdown faster than on that period. Eq. (4.16) is then expressed for an asymptotic period, T, as

$$\rho = \left(\frac{\Lambda}{T} + \sum_i \frac{\beta_i}{1 + \lambda_i T} \right) \tag{4.19}$$

Fuel element reactivity worth can be measured using a technique known as the positive period method. Such a method is advantageous in that it requires only the use of the core excess reactivity, i.e., all control rods fully withdrawn. It also eliminates the necessity for extra instrumentation to measure the reactivity worths of fuel elements. Additionally, it eliminates the effect of uncertainty in control rod calibration and in position indications of control rods. Positive period measurements are used with the inhour equation to determine the magnitude of the reactivity perturbation corresponding to the observed stable period.

It is important to note that there are bounds for using the positive period method. Such limits allow period measurements to be free of internal and external effects. However, the method is only applicable in the absence of temperature feedback caused by the inherent fuel moderator in KSU TRIGA fuel. Rising temperatures in the fuel cause the hydrogen in the fuel moderator (i.e., bound H) to oscillate, thus increasing the probability that a thermal neutron will gain energy in the lattice. This causes the thermal neutron spectrum to harden, causing a loss of reactivity due to decreased neutron absorption in ^{235}U. Additionally, rising temperatures in the fuel cause the capture resonances in ^{238}U to be broadened, known as the

Doppler effect, thus decreasing the resonance escape probability and resulting in a loss in reactivity in addition to requiring low fuel temperatures. The method also requires the absence of external sources of neutrons.

By evaluating a neutron flux or power signal for a given step reactivity insertion, the asymptotic period can be extracted to compute the reactivity using the inhour equation. The experimental procedure in the next section provides the setup for the positive period measurements. The power range used for these measurements, to avoid reactivity changes due to temperature feedback, is also discussed.

4.2 Experimental Configuration and Procedure

The positive period method was used at the KSU TRIGA MARK II reactor to determine the burnup of 26 out-of-core fuel elements. These elements have been used in the KSU core and were placed into the storage racks when replaced during changing configurations. The first set of measurements was performed in September 2015, for which six elements were selected, including a fresh element, to provide a burnup reference point. In March of 2016, 19 out-of-core fuel elements were used. There was prior knowledge that a slightly elevated xenon concentration had been in the core from the previous day of operation. The decision was made to measure these elements when it was initially thought that the concentration was negligible. However, it was later noted that xenon presence was high when a difference of 21 pcm in the core excess reactivity was measured in only an 8 hour interval. Therefore, these measurements were not included in the reactivity calculations of this work. Finally the last set of measurements were performed in May of 2016 which included a total of 26 out-of-core fuel elements, including the six elements performed in September 2015. Before starting the first and last set of measurements, the reactor had been shutdown for approximately 72 hours, which has sufficient to eliminate xenon effects on the reactivity measurements.

The procedure for these measurements began with a briefing from the Reactor Manager to the staff members about the fuel handling procedure to ensure that

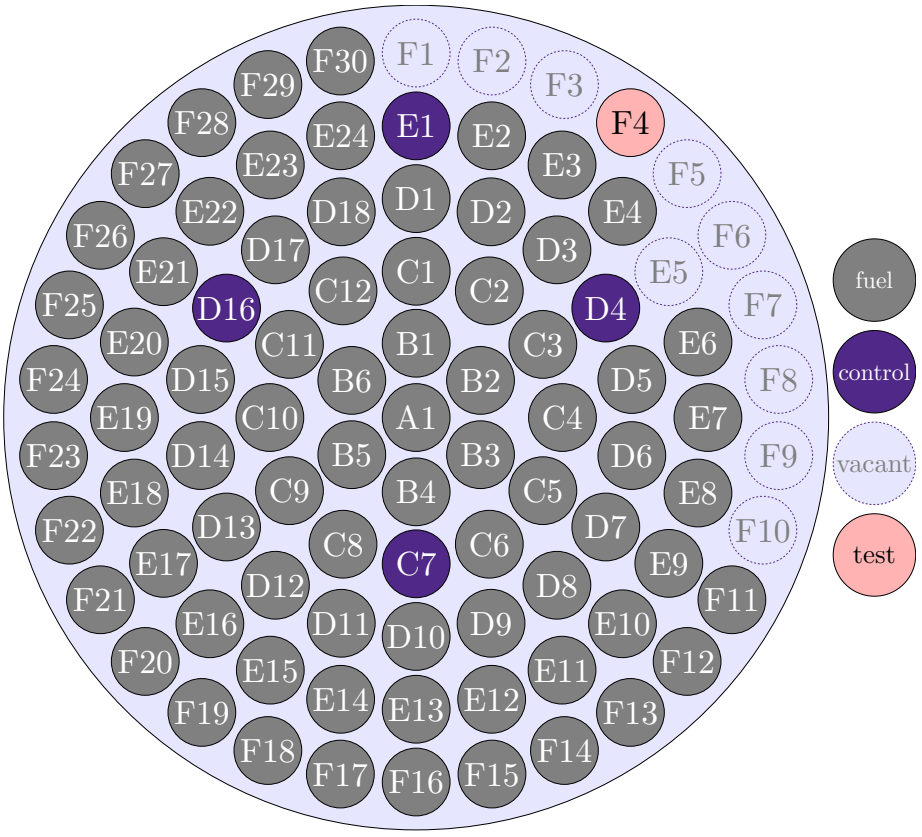

FIGURE 4.3: Core configuration for the reactivity method measurements

precautions and limits were implemented when moving fuel elements. A Senior Reactor operator (SRO) was notified to be present in the reactor bay for all fuel movements per fuel handling procedure. To establish a slightly supercritical core with all control rods withdrawn, nine fuel elements and the extraneous neutron source (Am,Be) from the F-ring and 1 fuel element from the E-ring were removed using the fuel handling tool. The core was established to be barely critical, so the period was small enough for the reactivity method with all rods withdrawn completely with a test element installed. The fuel elements and the source were placed in the racks available nearby in the reactor pool. A staff member in the control room was present to log the serial numbers of the fuel elements and their new rack locations. A survey meter was available for use during fuel movements to measure radiation levels at the pool surface. The core configuration for this experiment is depicted in Figure 4.3.

The achievement of a slightly supercritical core with fully withdrawn control rods allowed a first measurement of the excess reactivity of the new core. The

positive period method was conducted in three major steps to ensure a consistent methodology. First, three control rods (Pulse, Shim, Safety) were fully withdrawn and a fourth rod (Regulating) was withdrawn to the appropriate position to establish criticality at 1 W. The reactor operator then recorded the time and positions of these control rods in the logbook. Second, the fourth control rod was fully withdrawn and the positive period was observed. Third, the reactor operator scrammed the reactor, rapidly inserting all the control rods, when power reached 10 kW.

According to the KSU nuclear facility training manual, thermal feedback is absent roughly for thermal power less than 1000 W. However, the scram point was set at 10 kW to extract as much recorded data as possible. The exact point of thermal feedback was determined in later analysis by visual inspection of the power trend and verified by statistical analysis; see Chapter 5. The time-dependent power data for this first measurement was recorded by the strip chart recorder provided by the control console for the measurement. After that, the experimental position chosen was F-4, (see Figure 4.3) to avoid interfering with ongoing experiments in the reactor pool. As mentioned in Section 3.2.2, the experimental position in the past work was chosen in the C-ring, to have a gradient of neutron flux that was approximately constant. However, in this work, it was advisable to use an outer ring (e.g., E- or F-ring) for a test location in order to minimize the reactivity perturbation to facilitate a slow measurable period. The analysis of this effect is discussed further in Chapter 6. The minimization of reactivity perturbations increases the precision of positive period measurements and will reduce the likelihood of a period scram. The selected fuel element of interest was lowered into lattice position F-4 one by one and the same steps were taken for the measurements. At the conclusion of the procedure all fuel elements were returned to their starting locations in order to re-establish the prior core configuration.

Table 4.2: Stripchart Recorder.

Date	Time	NMP (% power range)	NLW (kW)	Fuel Temp (C)	NPP (% 1 MW)
5/23/2016	10:29:24	50.49133	0.9431407	19.48584	0.4691752
5/23/2016	10:29:25	50.49133	0.9431407	19.48584	0.4691752
5/23/2016	10:29:26	52.32051	0.9649889	19.61674	0.4746915
5/23/2016	10:29:27	53.44722	0.9857489	19.57934	0.4746915
5/23/2016	10:29:28	53.44722	0.9857489	19.57934	0.4746915
5/23/2016	10:29:29	54.98429	1.003435	19.46715	0.4802079
5/23/2016	10:29:30	56.95256	1.024745	19.59804	0.4802079
5/23/2016	10:29:31	56.95256	1.024745	19.59804	0.4802079

4.3 Experimental Data

The NLW, NMP, and NPP channels were available at the control console to report power versus time in the strip chart recorder. Table 4.2 illustrates the simple table format of the stripchart recorder, including the date, time, power indications, and the fuel temperature provided by a thermocouple element in one of the measurements. For the purposes of these measurements, only the NMP channel was used in the data analysis, since it was most valid for the range of power in the measurements. The NLW channel is a good indicator at low power but was invalid for these measurements since the readings were disrupted around 1 kW where the pulse mode changes automatically to a current mode. The NPP channel, which gives reading from 0-100% of 1 MW, was clearly invalid for these measurements because it gave 0% readings. The power ranges selected in the data analysis for the reactivity calculations is provided along with the burnup value of the each respective fuel element experimented within Chapter 5.

Chapter 5

Results

In this chapter, the inhour equation is used with the period measurements to determine reactivity. All analysis was performed using Serpent and MCNP with the ENDF/B-VII cross-section library. Python scripts were written to interpret the experimental and computational data.

5.1 Period Measurements

Recall that the neutron population P in a delayed supercritical nuclear reactor is well described by a single exponential in the asymptotic regime, i.e., $P \propto \exp(t/\tau)$, where τ is the period and t is the time. The stripchart recorder was used to extract the time-dependent data of all control rods out core with 26 out-of-core tested fuel elements. Data recorded by the NMP channel as percent power was converted to absolute power in kW for analysis. The top portion of Fig. 5.1 shows the NMP channel's power and a corresponding linear regression model of a fall 2015 period measurement of fuel element 6578 by the least squares method, where the slope is taken as the inverse period.

As observed in the figure, the period stabilizes (i.e., becomes asymptotic) at around 65 seconds. The bottom portion of Fig. 5.1 shows a normal probability plot of the model error (t> 65 seconds) for the same tested element. These percent

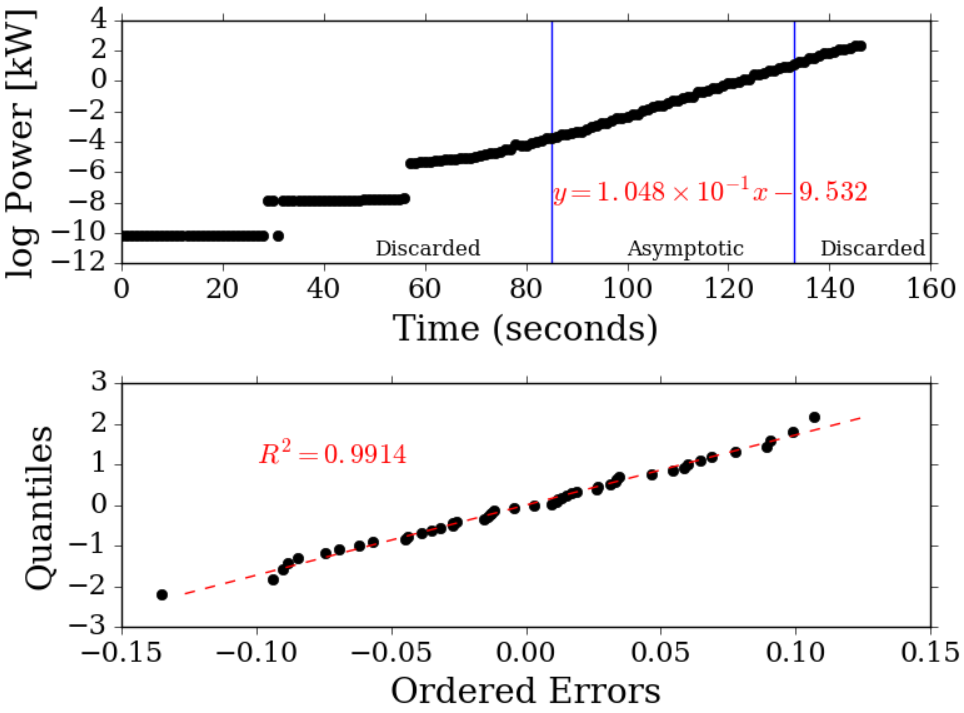

FIGURE 5.1: NMP channel's (compensated ion chamber), power vs time for fuel element 6578.

differences were examined by the Anderson-Darling Normality test, a statistical test used to determine if data is drawn from a normal probability distribution. The coefficient of determination, a statistical measure of how well the regression line approximates the data points, was found to be 0.9914[17]. In order to extract the asymptotic or stable period for all measurements, lower and upper bounds of the time dependent power data were set for all the measurements to avoid any distribution to the asymptotic behavior of period measurements. A conservative lower bound was set at 50 W, since loss of sensitivity on the NMP channel was observed below about 4 W. As mentioned in Section 4.2, the thermal feedback for the KSU reactor is observed above 1 kW, however an upper bound was set at 2 kW based on visual inspection of thermal feedback of power data for all 26 fuel elements. The same bounds were selected for all the time dependent power data to maintain consistency. Table 5.1 shows the period for all fuel elements tested with their respective uncertainties. These periods are used in the inhour equation Eq. (4.19) later in this chapter to calculate reactivity worths for all the fuel elements. However, first the delayed neutron data for each tested fuel element

Table 5.1: Asymptotic period measurements.

Test Element	Measurement 2015	Day 1 2016	Day 2 2016	Day 3 2016
Vacant	27.45 ± 0.097	41.673 ± 0.066	40.095 ± 0.061	36.738 ± 0.071
11352	9.293 ± 0.082	NA	12.515 ± 0.094	NA
6578	9.535 ± 0.069	NA	12.748 ± 0.089	NA
4349	9.685 ± 0.074	13.653 ± 0.063	NA	NA
4339	10.086 ± 0.070	13.712 ± 0.071	NA	NA
5254	10.272 ± 0.081	NA	14.318 ± 0.084	NA
5031	10.591 ± 0.087	NA	14.330 ± 0.064	NA
3684	NA	15.015 ± 0.089	NA	NA
4078	NA	14.513 ± 0.082	NA	NA
4080	NA	14.997 ± 0.119	NA	NA
4102	NA	14.311 ± 0.100	NA	NA
4143	NA	13.804 ± 0.071	NA	NA
5019	NA	14.082 ± 0.072	NA	NA
5253	NA	14.340 ± 0.068	NA	NA
2942	NA	NA	12.787 ± 0.091	NA
2982	NA	NA	13.072 ± 0.083	NA
5039	NA	NA	14.318 ± 0.083	NA
5647	NA	NA	14.187 ± 0.082	NA
5654	NA	NA	13.896 ± 0.068	NA
5947	NA	NA	13.596 ± 0.087	NA
5950	NA	NA	13.765 ± 0.068	NA
5951	NA	NA	13.333 ± 0.084	NA
2425	NA	NA	NA	12.735 ± 0.082
2788	NA	NA	NA	12.041 ± 0.072
2789	NA	NA	NA	11.801 ± 0.072
2937	NA	NA	NA	11.681 ± 0.072
4072	NA	NA	NA	13.003 ± 0.060

is required for these calculations. Kinetics parameters needed for evaluation of the inhour equation can be found using the adjoint-weighting features of MCNP6. In order to extract the delayed neutron data, models from MCNP and Serpent was used to perform step-burnup calculations in order to properly model the present core configuration starting from the initial loading of SS clad fuel.

5.2 Serpent Isotopic Composition

Serpent, a three-dimensional, continuous-energy Monte Carlo code, was used to evaluate the burnup compositions of KSU TRIGA Fuel[6]. Fuel elements as mentioned before in Section 2.1 are arranged in rings which meant that a representative repetitive fragment of the large reactor lattice, known as a unit cell,

can be modeled[18]. A unit cell is composed of a single fuel element surrounded by a moderator portion where the boundary is set in the middle of the moderator dividing the nearest fuel elements. To be able to identify the representative reactor lattice in the model, evaluation of the geometry of the KSU core was made. It was found that there are fuel elements arranged in both square and hexagonal lattices where fuel elements are situated in corners of squares and hexagons, respectively. Later analysis in this section to compare burnup compositions of a square and hexagonal-pitch unit cell model in Serpent showed indifference to the type of unit cell used. Therefore a square-pitch unit cell used as the model approach was appropriate to use for input material definitions in MCNP.

Fuel that was used inside the KSU reactor was defined in the model based on the fuel description described in Section 2.1. Figure 5.2 depicts the view section of a single square-pitch unit cell that was used for a 3-D axial discretization of 7 fuel regions and a single radial region. The lattice pitch, the distance between centers of direct neighbors of fuel elements, was averaged over the entire core to determine the unit cell boundary distance. As mentioned in Section 1.1, this work will emphasize the effectiveness of modeling only the axial burnup dependence on reactivity. This is a reasonable approach because defining fuel compositions as continuous functions of z,r,θ for each element would most likely be impossible and ongoing work suggests little dependence on r for unit-cell studies[5]. Furthermore, 7 regions of axial discretization is sufficient enough to eliminate reactivity biases due to material evolution[5].

It is important to note that the 3-D fuel model is symmetric about Fuel 1, hence all discretization used results of fuel materials 1, 2, 3, 4, see Figure 5.2[5]. Reflective boundary conditions were made in the Serpent model in an infinite moderator lattice in the top and bottom of the fuel pin. A series of burnup steps were made in the Serpent model to produce composition data in the range of 0-50 MWD/kg(U). The cross section libraries were chosen based on a uniform temperature of 600 K for the fuel materials. In all cases, 50 inactive cycles and 500 active cycles with 20,000 histories per cycle were used for each burnup step. Selection of major actinides and fission products were made to track during the simulation. These dominant

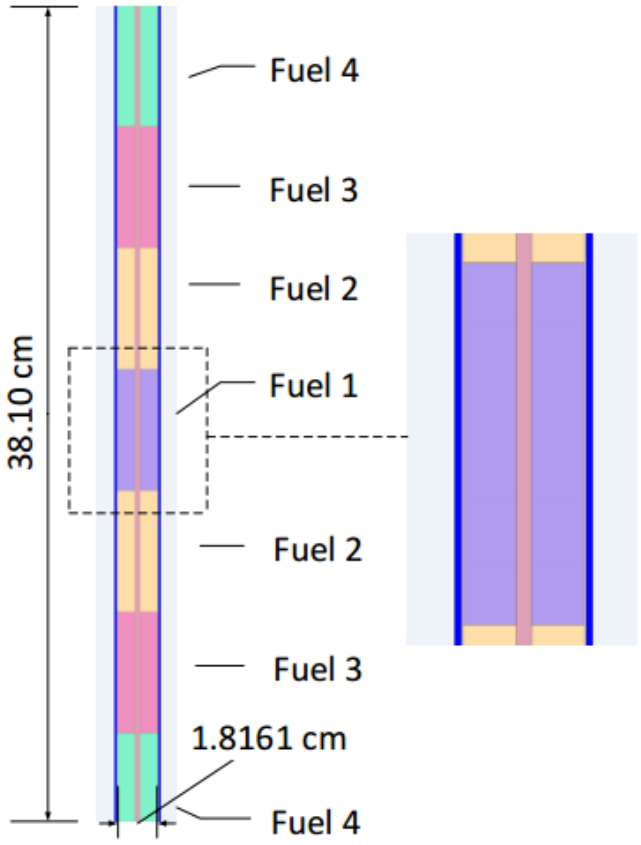

FIGURE 5.2: Model of 7 axial discretization of KSU TRIGA fuel[5].

isotopes were selected based on the efficiency of their ability to absorb neutrons. According to the sensitivity analysis performed by Oak Ridge National Laboratory on burnup credit for PWR spent fuel[19] and the sensitivity analysis mentioned in Section 3.2.3, the isotopes are: ^{234}U, ^{235}U, ^{236}U, ^{238}U, ^{238}Pu, ^{239}Pu, ^{240}Pu, ^{241}Pu, ^{242}Pu, ^{241}Am, ^{243}Am, ^{237}Np, ^{99}Tc, ^{133}Cs, ^{135}Cs, ^{143}Nd, ^{145}Nd, ^{147}Sm, ^{149}Sm, ^{150}Sm, ^{151}Sm, ^{152}Sm, ^{153}Eu, ^{155}Gd, ^{95}Mo, ^{154}Eu, ^{135}Xe, ^{147}Pm, ^{131}Xe, and ^{103}Rh.

Figure 5.3 illustrates the importance of Pu, a vital isotope for fission reactions, production as a function burnup. The Serpent model shows that a TRIGA fuel element that has a burnup of 6 g of original ^{235}U would lead to approximately 0.45 g of ^{239}Pu produced. In order to extract the compositional data prior to the initial loading of the SS clad fuel inside the KSU reactor, the initial burnups of ^{235}U in grams were converted to MWD/kg(U) using the procedure in Appendix A. The compositional data was later interpreted to write the material definition for MCNP

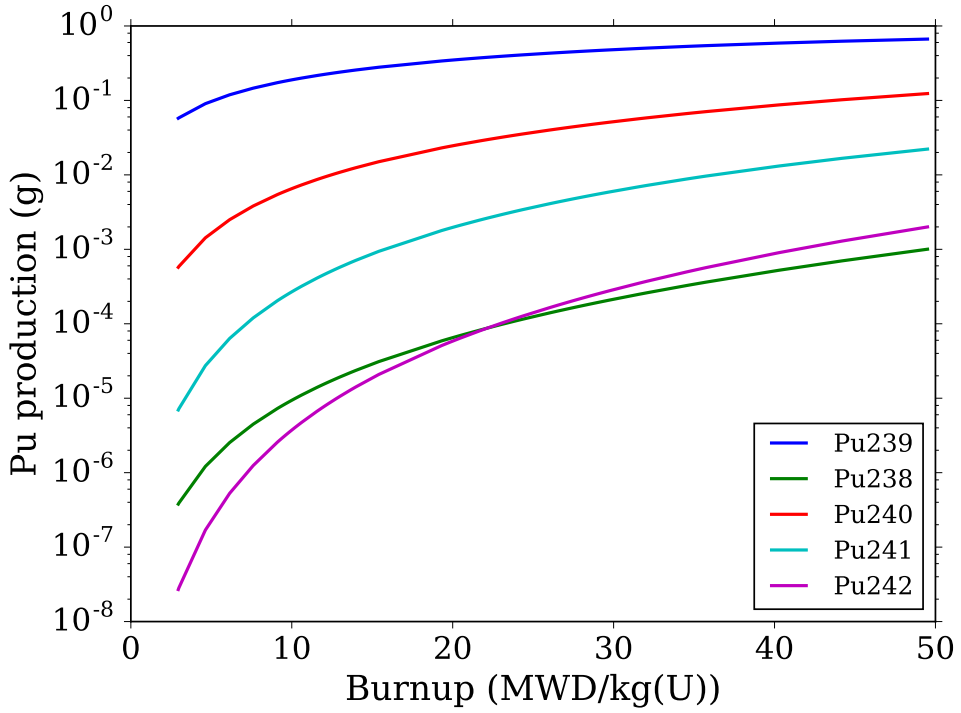

FIGURE 5.3: Pu growth as a function of burnup.

input files. The burnup of all KSU TRIGA fuel was estimated using the power peaking factor calculations in MCNP using an F7 tally. This will be described in more detail in the next section.

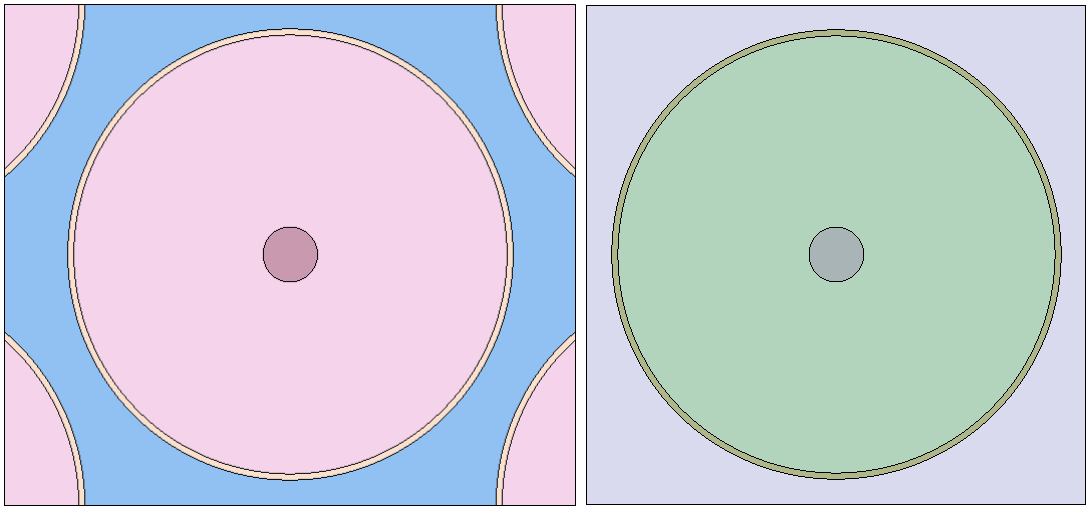

(A) Hexagonal (B) Square

FIGURE 5.4: Hexagonal and square Pitch unit cell Serpent models[5].

A comparative analysis explored the difference between a square-pitch unit cell and a hexagonal-pitch unit cell model for composition inputs in MCNP kcode

TABLE 5.2: Hexagonal vs square pitch unit cell model.

Parameters	Hexagonal	σ (%)	Square	σ (%)
k_{eff}	1.08597	0.00280	1.08573	0.00284
ρ (pcm)	7916.49	20.00	7895.90	20.00

calculations. Figure 5.4 shows both the hexagonal and the square pitch unit cell Serpent models. 50 cases of MCNP files were run for this analysis, 25 for each unit cell type used for input material definitions, with different initial seed numbers. All cases were run with 30 inactive cycles and 250 active cycles with 100,000 histories per cycle. Table 5.2 provides both the modeled k_{eff} and the excess reactivity for the unit cell definitions. By observing the variations of k_{eff} and ρ in the MCNP model of configuration Core III-7 with control rods withdrawn, it was determined that the overall effect of k_{eff} and ρ were indifferent to the type of unit cell modeled in Serpent.

5.3 Power Peaking Factors

As mentioned in Section 1.2, the current methodology performed by the KSU reactor staff to estimate spent fuel burnup suffers from large uncertainties. In order to maintain consistency with the fuel-inventories method of estimating burnup, see Eq. (2.1), power peaking factors of the KSU core were calculated using an F7 tally in MCNP[7]. The F7 tally which produces results in the fission power in MeV/g per source particle released in each cell is used to calculate the power peaking factor by taking the ratio of local to average power density in each fuel element, starting with the first core configuration in 1973. The integrated energy produced for each core configuration, taken from the logbooks, in combination with the power peaking factors are used to estimate the burnup of individual elements. The Serpent model was used again to interpret the new compositional data based upon those burnup values for the next core configuration and the sequence was repeated until the current configuration. The patterns, and subsequent changes in the core configurations, were used to update the burnup of all fuel elements in

the core's history, as shown in Figure 5.5. Control rods were fully withdrawn in the MCNP model to eliminate reactivity biases from control rods in the power peaking factor calculations. In all cases, 30 inactive cycles and 250 active cycles with 100,000 histories per cycle were used for each core step.

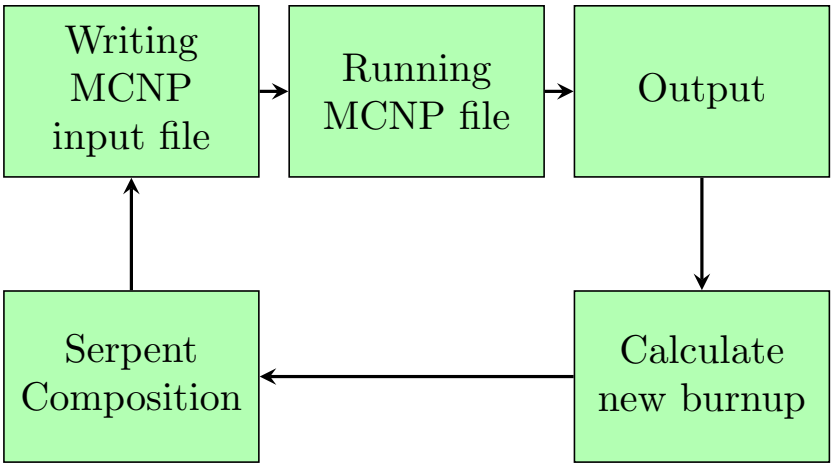

FIGURE 5.5: Flow chart for the Python script used for burnup calculations.

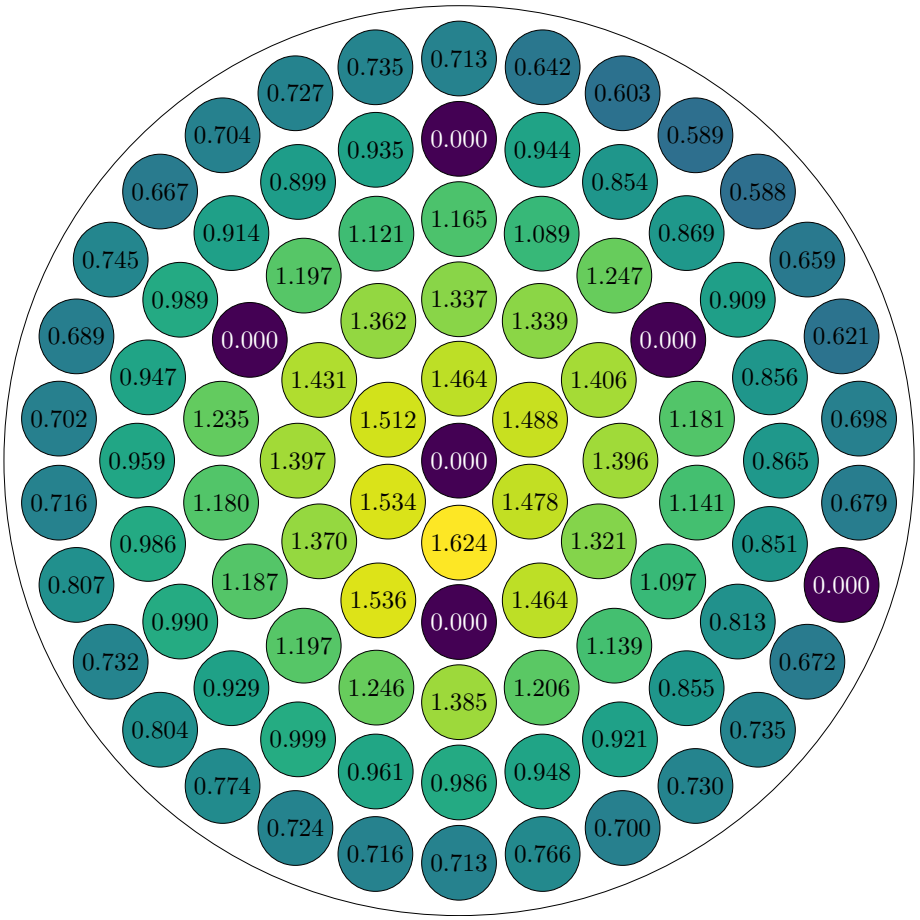

FIGURE 5.6: Core III-7 element averaged power peaking factor plot.

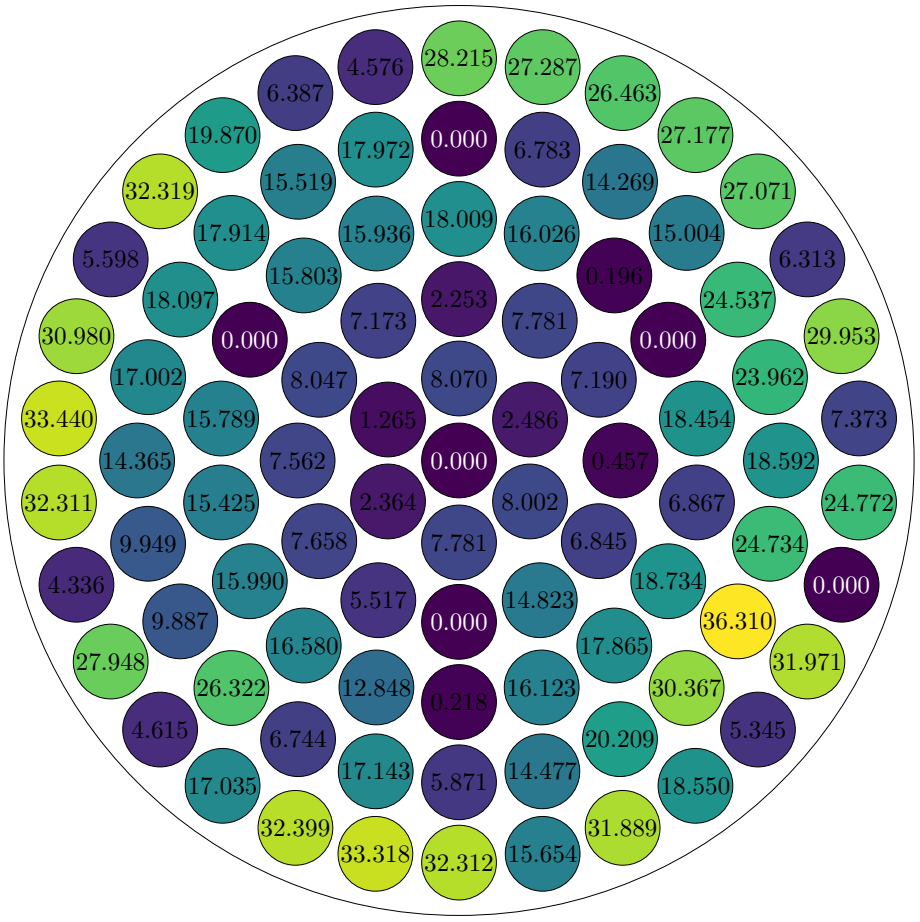

FIGURE 5.7: Estimated total burnups in $\frac{MWD}{kg(U)}$ for Core III-7.

Two power peaking factor methods were examined in determining the total burnup of several fuel elements. The first case was to use the ring averaged power peaking factor. The second case was to use the specific element power peaking factor. In both cases, the axial discretization tallies were averaged for a single fuel element. The fuel elements chosen for this examination conveniently remained in the same locations since their first loading in the KSU core.. Figure 5.6 depicts the element averaged power peaking factors plot for the Core III-7 while Figure 5.7 shows the estimated total burnups for those elements. These two cases were compared to the methodology used by the KSU staff for analysis. Table 5.3 provides both cases respective to the fuel elements' accumulated burnup and position at KSU.

It is evident that the current methodology performed by the KSU staff suffers from large errors in element-wise burnups, especially for fuel elements closer to the center of the core, where higher neutron flux occurs. In the cases of fuel elements 6315

Table 5.3: Accumulated burnup for three methods.

Position	Fuel ID	KSU method MWD/kg(U)	Element Pf method MWD/kg(U)	Ring Pf method MWD/kg(U)	Ring-Core (%)	Element-Core (%)
B1	6315	5.388	8.069	8.185	-51.897	-49.755
B2	10880	1.667	2.485	2.530	-51.743	-49.043
B5	10895	1.528	2.363	2.318	-51.749	-54.677
B6	11341	0.825	1.265	1.253	-51.794	-53.211
C1	11351	1.667	2.253	2.330	-39.715	-35.084
C2	6316	5.388	7.781	7.474	-38.710	-44.398
D1	3380	5.388	6.183	6.309	-17.069	-14.751
D2	3330	5.388	6.111	6.309	-17.069	-13.419
D11	2435	5.388	6.707	6.309	-17.069	-24.472
E4	3006	5.388	4.786	4.895	9.165	11.184
E12	3690	5.388	5.140	4.895	9.165	4.608
F1	5017	5.388	3.874	3.691	31.512	28.108
F2	5018	5.388	3.545	3.691	31.512	34.222
F3	5027	5.388	3.408	3.691	31.512	36.751
F4	5021	5.388	3.310	3.691	31.512	38.574
F5	5026	5.388	3.282	3.691	31.512	39.100
F14	5653	5.388	3.776	3.691	31.512	29.936

and 6316, fresh at the time of loading, the current methodology under-predicts the accumulated burnup by approximately 50% and 40% for both power factor methods. These differences generally decrease for D and E elements but is increased for F ring elements, where the accumulated burnup is over-predicted by approximately 30% for both power factor methods. For the purposes of this work, the second case was used to individually assess the burnup of each fuel element to accurately model the current configuration.

5.4 Test cases for burnup sampling and kinetics parameters

According to the power peaking factor calculations, the KSU method is unfit to properly quantify spent fuel compositions. The element position power factor method is well suited to estimate the burnup of the KSU fuel, though. Note, however, that initial burnup estimations made prior to installation at KSU used ring-averaged power peaking values, see Eq. (2.1). In order to quantify the overall uncertainties associated with the current composition in the KSU fuel, the percent differences between the two power factor methods were further analyzed.

Percent differences between the two power factors were made for all the elements' accumulated burnup during their respective time in the KSU core. This allowed a comparison between the two methods, which provided an estimate of the errors associated with the ring averaged power peaking factors used in Eq. (2.1). These percent differences were later examined by the Anderson-Darling Normality test. The data was then determined to follow a normal distribution, where the coefficient of determination is 0.9859. Figure 5.8 shows the normal probability plot of all the fuel elements percent differences between the two cases.

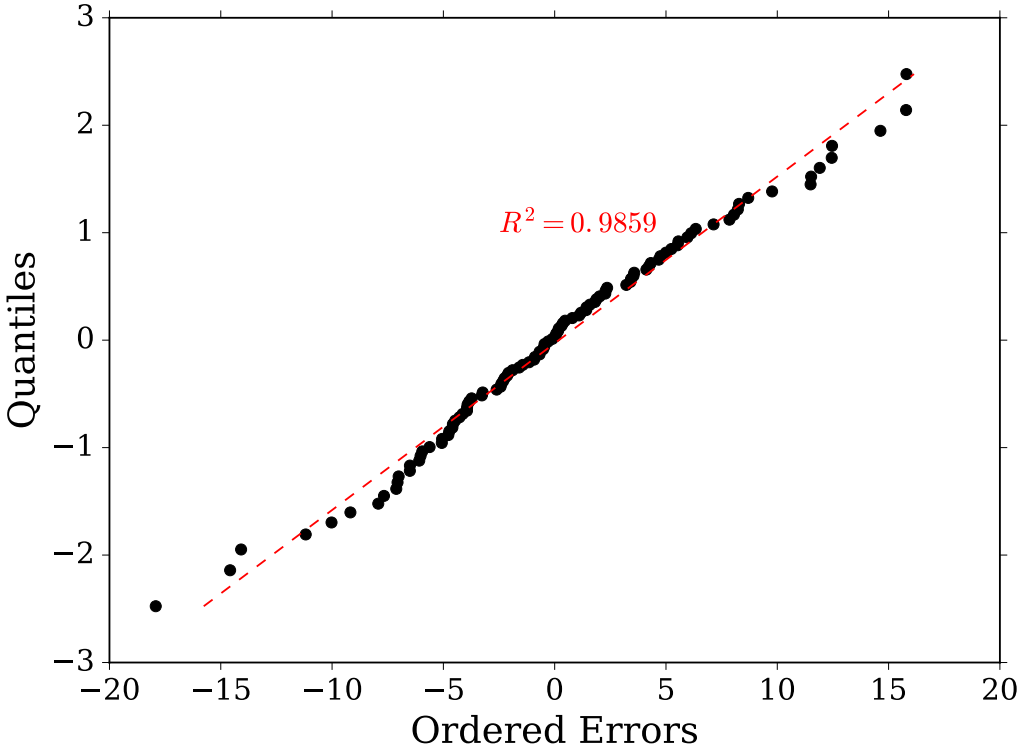

FIGURE 5.8: Normality plot of errors in the two power factor methods.

In order to accurately represent the uncertainties associated with the initial burnup, 200 test simulations were performed and investigated. From the distribution of the errors, initial burnups of elements for the initial configuration back in 1973 were sampled. Burnups were sampled using assumed ring-averaged total burnup values, from the shipment documents, with an associated error value sampled from the error distribution, see Eq. (5.1),

$$BU_{SI_i} = BU_{RI_i}\,(1+\eta) \tag{5.1}$$

where BU_{SI_i} is the initial burnup for element i, BU_{RI_i} is the assumed initial burnup value for element i based on the ring-averaged power peaking factor, and η is the percent error sampled from the error distribution.

200 file cases were made such that the initial burnup values for each element in the initial core configuration was sampled individually. These burnup samples were then used to generate 200 MCNP input files to run a sequence of burnup steps, starting with the initial core configuration in 1973 until Core III-7. Much like the procedure described previously, the power peaking factor method was used to calculate the new burnup in each changing configuration. The file cases were automatically updated by the Python script, see Section 5.3, with each burnup step. In all cases, 30 inactive cycles and 250 active cycles with 10,000 histories per cycle were used for each core step. The number of histories per cycle were lowered in order to reduce computational time. The final output of the 200 files was an estimated total burnup value for each element that has been in the KSU core.

By comparing the variations of the 200 total burnup values for each element to its average total burnup values, one could determine the type of the distribution in the error differences. Since fewer histories were used for the generation of the 200 output files, the uncertainties associated with the power factors in the MCNP models are increased compared to calculations performed in Section 5.3. Regardless, it has been determined that the error differences between total burnup values using both power methods are reasonably well represented by a normal distribution, as shown in Figure 5.9.

Note that the error distribution does not account for the errors from the fuel's compositions prior to usage at KSU. There is little information about the fuel surroundings, i.e., mixed fuel, control rods, etc., prior to installation at KSU which could lead to deviations in the axial compositions and reactivity worths. Fortunately, linear expectations from the reactivity worth measurements based on total burnup estimations could identify the deviations of a fuel element's worth from those modeled by MCNP as presented in the next section. From the 200 output files of total burnups, the experimental core configuration described in

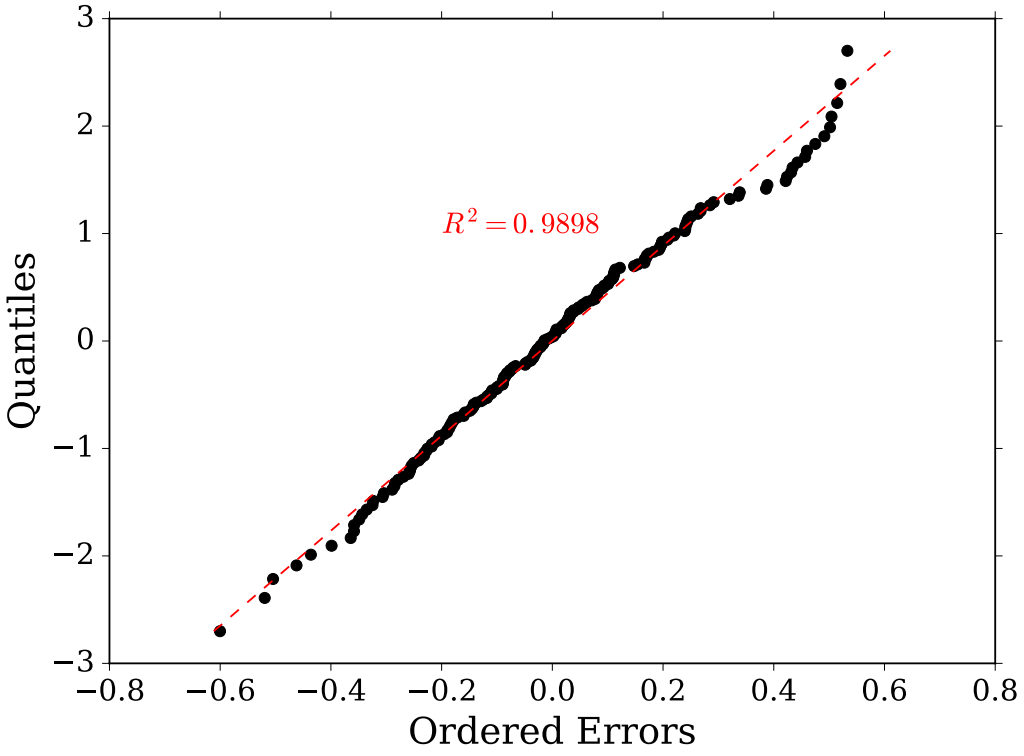

FIGURE 5.9: Normality plot of error differences in 200 burnup values to its average for fuel element 6578.

Section 4.2, was modeled in MCNP for vacancy in the test location as well as for the 26 tested fuel elements selected for this work. The output of these MCNP file simulations is k_{eff} from which reactivity is computed via Eq. (3.1) for modeled reactivity worth comparisons. Additionally, the kinetics parameters needed for evaluation of the inhour equation were found using the new adjoint-weighting features of MCNP. Table 5.4 shows an example of the 6 precursor groups produced by MCNP.

TABLE 5.4: An example of kinetics parameters from MCNP.

precursor	β_{eff}	std. dev.	energy (MeV)	std. dev.	λ_i (/sec)	std. dev.	half-life (sec)
1	0.00021	0.00001	0.40347	0.00150	0.01249	0.00000	55.49352
2	0.00116	0.00003	0.47190	0.00068	0.03180	0.00000	21.79599
3	0.00119	0.00004	0.44290	0.00067	0.10940	0.00000	6.33582
4	0.00326	0.00006	0.55654	0.00053	0.31718	0.00000	2.18537
5	0.00099	0.00003	0.51665	0.00102	1.35345	0.00002	0.51213
6	0.00034	0.00002	0.54175	0.00191	8.65215	0.00066	0.08011

5.5 Reactivity worth calculations

As mentioned in Section 4.2, only period measurements of September 2015 and May 2016 were considered for this work. The period measurements were and kinetics parameters extracted from MCNP were used for the inhour equation, (Eq. (4.16)) for experimental reactivity worth calculations. Not only did the initial sampling of the 200 input burnups in the MCNP files create total burnups of all fuel elements and its uncertainties, but it also provided the opportunity to model 200 experimental core configurations for which 200 modeled and experimental reactivity worths were evaluated for the 26 tested fuel elements. Table 5.5 shows the total burnup of 26 out-of-core fuel elements, the modeled and experimental reactivity worths, and their associated uncertainties from the variation of the 200 values. Appendix B provides estimated total burnups for all fuel elements used in the KSU core. Figure 5.10 illustrates all the experimental and modeling efforts for this work.

TABLE 5.5: Table of burnup and reactivity worths of the tested 26 fuel elements.

Fuel ID	burnup MWD/kg(U)	σ %	September 2015 pcm	σ pcm	May 2016 pcm	σ pcm	Modeled pcm	σ pcm	Fall-modeled pcm	Spring-modeled pcm
11352	0	0	114.56	0.99	110.67	0.87	117.51	1.36	-2.95	-6.83
2937	2.92	6.00	NA	NA	100.96	0.89	110.23	1.36	NA	-9.27
2982	2.94	7.10	NA	NA	106.11	0.86	102.90	1.36	NA	3.21
2942	2.95	6.35	NA	NA	108.03	0.86	107.68	1.36	NA	0.35
6578	6.02	0.22	111.42	0.98	108.54	0.86	108.31	1.36	3.12	0.23
2788	7.23	3.28	NA	NA	102.12	0.89	114.10	1.36	NA	-11.99
2425	13.68	5.00	NA	NA	101.61	0.87	103.53	1.36	NA	-1.92
2789	15.04	5.20	NA	NA	101.67	0.89	105.53	1.36	NA	-3.86
5039	22.25	6.65	NA	NA	95.53	0.83	101.49	1.36	NA	-5.97
4339	23.29	5.78	103.78	0.97	102.49	0.84	100.71	1.37	3.07	1.78
4349	23.72	5.59	110.77	0.98	104.89	0.85	103.98	1.36	6.78	0.91
5254	26.95	5.22	101.92	0.96	95.14	0.83	100.60	1.36	1.32	-5.46
5950	28.36	6.85	NA	NA	99.24	0.84	100.11	1.36	NA	-0.87
5019	29.01	6.18	NA	NA	100.27	0.83	96.81	1.36	NA	3.46
4102	29.20	6.52	NA	NA	98.88	0.83	98.66	1.36	NA	0.21
5951	29.58	5.76	NA	NA	102.58	0.85	98.82	1.36	NA	3.77
5947	29.70	6.01	NA	NA	101.47	0.85	96.66	1.36	NA	4.82
5654	29.84	6.14	NA	NA	99.67	0.84	98.41	1.36	NA	1.26
5031	30.71	5.67	98.86	0.96	95.45	0.83	101.01	1.36	-2.15	-5.56
5647	31.59	6.54	NA	NA	96.91	0.84	95.89	1.36	NA	1.03
5253	35.17	6.26	NA	NA	98.36	0.83	93.70	1.36	NA	4.66
4080	35.68	6.19	NA	NA	92.19	0.81	93.26	1.37	NA	-1.08
4072	38.48	5.61	NA	NA	101.70	0.87	92.54	1.36	NA	9.16
4143	40.73	6.39	NA	NA	104.00	0.84	93.37	1.36	NA	10.63
3684	44.63	6.97	NA	NA	92.45	0.81	91.82	1.36	NA	0.63
4078	49.10	6.19	NA	NA	97.03	0.83	88.30	1.37	NA	8.73

As shown in Table 5.5, a large number of measured reactivity worths differ from those modeled. The overall trend of both the experimental and modeling efforts suggest that reactivity and burnup have an inverse linear relationship, confirming

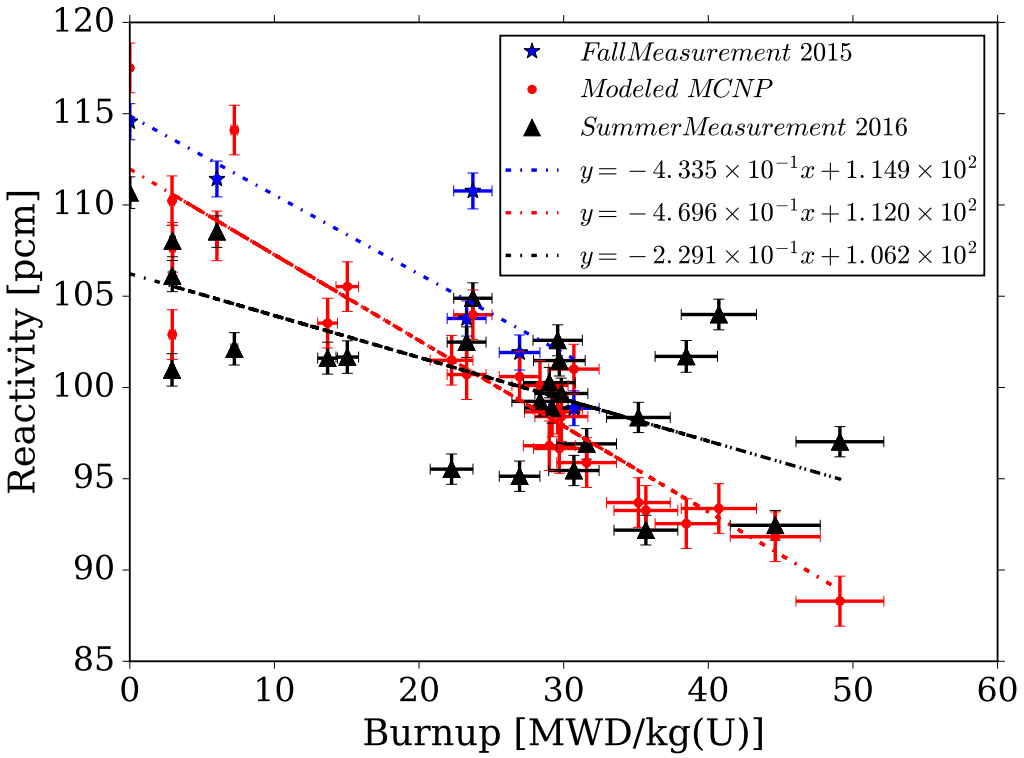

FIGURE 5.10: Reactivity vs Burnup for KSU TRIGA fuel.

previous work; recall Figure 3.1. By comparing the September 2015 and May 2016 measurements, there exists a constant bias where the worths of the 2015 measurements are higher for the 6 tested fuel elements. According to the experimental measurements performed on Day 1 and 2 of 2016, there exists a decrease of approximately 5 s and 3 s in period measurements of the core configuration at vacancy during an 8 hour period, respectively. The excess reactivity difference that lead to this change was approximately a gain of 10 pcm and 6 pcm between the two periods. Day 3 did not experience such a difference. It was suspected during the evaluation of this bias, that there might be instrumental errors on the NMP channel. For sanity, the NLW power data was used to determine the period measurements to observe any bias. Although the NLW power data does not provide the correct magnitude of the period measurements, evaluations was made for its time-dependent power asymptotic regime during the 8 hour difference. It too showed a decrease in the period measurements of 5s and 6s for Days 1 and 2, respectively, while no such difference was observed for Day 3. This suggests that the suspected instrumental errors on the NMP channel could not have been the

cause for such a difference. This is confirmed by approximate loss of reactivity between the 2015 and Day 3 measurements. The increase of approximately 10s, from 27.45s to 36.74, which led to a decrease of approximately 25 pcm, in the period measurements for a vacant position between the measurement in 2015 and Day 3 of 2016. This was validated by modeling the two measurements in which integrated energy produced between the 2015 measurements and 2016 measurements, approximately 1.33 MWD, was accounted for in the fuel burnup. This contribution of integrated burnup led the difference between the modeled worths of the two measurements to be approximately 21 pcm. This indicates that there might be unresolved core conditions existing for measurements performed on Days 1 and 2. As previously implied, the Xe effects are eliminated as a potential cause, since there were not any operations for 72 hours prior to the measurements. The logbook data also showed that the last two operational days prior to the awaiting period of 72 hours was kept at approximately 10 W, "zero-power region", at critical log sets, implying that there is a definite elimination of the potential cause arising from Xe effects. By examining the fuel temperature responses during the measurements, it was also concluded that any rise in temperatures would have a negative response in reactivity, so this was also eliminated as a potential cause. There is, however, a positive response to moderator temperatures rising but this was not considered as a significant factor because they did not rise during critical log sets. Furthermore, the pool coefficient of reactivity is very small in TRIGA reactors, 0.05 $\frac{\dot{\mathrm{c}}}{^{\circ}C}$ [8] and therefore could not have been the cause. The specific bias is yet to be determined after eliminating several potential causes.

By comparing the modeled worths to the experimental worths on Day 3, there were a few elements that suggest another reason for the reactivity biases observed in this work. Higher burned fuel element, e.q., 4072, 4143, 4078, suffer from large biases from their respective modeled worths. Since there is an unclear cause for the measurement biases observed on Days 1 and 2, the measurement of fuel element 4072 which was performed on Day 3 can give a clearer insight on biases observed for those higher burned elements. The background history of these elements prior to installation at KSU is unknown, and therefore it is probable that they spent most

of their core lifetimes in different conditions experiencing high flux irregularities during their lifetimes prior to installation at the KSU core. This suggests that the differences could be caused by the orientation of these specific fuel elements during the period measurements. Note that orientation of fuel elements surrounding the test location during the measurements, i.e., in E-3 and E-4, remained the same and thus is not a reason for any biases observed in this work. Furthermore, the same reason is said of fuel element 2788. This specific fuel element had received minor burnup prior to use at KSU, however, upon reviewing its surroundings at the KSU core, the bias observed between the measured and modeled worths could be explained by its lifetime near the Shim rod.

Chapter 6

Conclusion and Future Work

6.1 Summary

The overarching goal of this work was to provide KSU reactor researchers with new experimental benchmark data to produce a detailed model of the KSU reactor core. This work has pursued the reactivity method as one nondestructive technique to understand current KSU reactor fuel composition. The technique allows an indirect estimation of burnup and composition of fuel based on the assumption that reactivity is a known function of burnup. Since the technique allows only relative reactivity differences, a minimum of two fuel elements with well-specified burnups must be available to define a relationship between reactivity and burnup. The motivation for this work was to provide the KSU staff with a reliable method for determining burnup. In particular, it was noted that the current methodology, which suffers from great uncertainties due to inaccurate approximations, is not suitable for determining element-integrated values of burnup. Moreover, since the majority of the KSU TRIGA fuel was depleted prior to installation at KSU, it was important that these values served as measurable data points in the reactivity measurements.

As an alternative, the standard report outlined in Chapter 2, which provided the estimation of burnup prior to KSU usage, was taken as the method to estimate

the additional depletion at KSU to maintain consistency. A literature review was developed, which took into account the expected trend between reactivity and burnup for TRIGA fuel in Chapter 3. For a 8.5 wt % SS TRIGA fuel, like that of KSU fuel, a linear correlation was expected. The positive period method was also discussed to measure asymptotic or stable periods for which reactivity could be solved via the inhour equation. Furthermore, a study was reviewed to determine the isotopic composition importance for TRIGA fuel during depletion. These isotopes were later incorporated in a Serpent model of KSU TRIGA fuel to track its concentration as a function of burnup.

Thereafter, the experimental procedure and setup of the KSU core configuration for a slightly supercritical core with all control rods withdrawn for the positive period measurements was developed in Chapter 4. Only measurements with no Xe presence were considered for this work. The excess reactivity of the core allowed reactivity worth difference to be computed for all tested fuel elements. Furthermore, only the NMP channel (compensated ion chamber) was used in the data analysis since it was the most valid for the range of power in the measurements. Time-dependent power data extracted from the stripchart recorder was used to determine the asymptotic period to compute reactivity. The inhour equation was derived earlier in Chapter 4 to provide the relationship between asymptotic period and reactivity. The extraction accounted for the lower and upper bound set in the transient response to eliminate the reactivity disruptions due to loss of sensitivity on the NMP channel and avoid thermal feedback. The kinetics parameters needed to compute the experimental reactivity worths were found using modeling in MCNP.

Serpent was used to model the KSU TRIGA fuel as a square-pitch unit cell with 7 discrete axial fuel regions, the minimum number of fuel regions to eliminate reactivity biases due to material evolution. Thereafter, isotopic composition was available in the range of 0-50 MWD/kg(U). As an example, Pu production as a function of burnup were determined from the model. Burnup step procedures began by defining the material composition of initial loading of fuel at KSU in 1973 using Serpent. To account for the burnup steps throughout changing core patterns at KSU, a Python script was used to input material definition cards from Serpent into

MCNP files. A procedure for determining total burnup of the KSU TRIGA fuel was developed using the F7 tally provided by MCNP to compute power peaking factors methods. The procedure took into account two power peaking factor methods; one by using local cell values and another by ring-averaged values. The percent differences of accumulated burnup at KSU from using the two methods allowed burnup sampling for 200 test simulations of initial burnup prior to installation at KSU. This is due to the accurate representation of the uncertainties associated with the ring-averaged power factor method.

Finally, ρ values were provided as a function of burnup from the model and the experiments. It was observed that the overall correlation of reactivity to burnup was linear. However, large reactivity biases were observed, especially for three highly burned fuel elements whose historical surrounding at previous facilities is unknown. The reactivity bias observed in this elements was most likely due to the unknown radial orientation of tested fuel elements, as was reported in previous work[3]. Biases observed between the measurements of 2015 and 2016 is unclear after eliminating potential biases, though it suggests core conditions were the primary reason for the observed increased in excess reactivities.

6.2 Future Work

The work described in this thesis addresses the importance of quantifying burnup and composition. There are a few direct extensions of work that would be of substantial value to this area of research. Some of the key points of interest are:

- Verifying total burnup values. Gamma spectroscopy is a direct method of determining burnup, and hence will serve as validation for the reactivity method implemented in this work.
- A much more thorough period re-measurement should be made with known fuel orientation. Furthermore, re-measurements of the same fuel elements in the same day should be made to observe any biases due to core conditions.

- More work should be performed to model the KSU TRIGA fuel. In particular, graphite spacers should be added to the Serpent model at the top and bottom of fuel segments to observe the compositional changes with increasing burnup.

- More work should be performed to quantify the uncertainties in the logbook data. Both the log data and the strip-chart recorder are limited by the uncertainties in the instruments. However, the logbook in addition is also limited by the uncertainty arising from the operator recording the data. The difference between the reactor staff method and power generation per second from the strip-chart recorder could help quantify the uncertainties in the burnup calculation.

Bibliography

[1] Triga mark iii reactor description. Technical report, Gulf General Atomic, 1968.

[2] M. Ravnik, A. Trkov, I. Mele, and M. Strebl. Determination of the burn-up of triga fuel elements by calculation and reactivity experiments. *Kerntechnik (1987)*, 57(5):291–295, 1992.

[3] A Persic, M Ravnik, and T Zagar. Burn-up triga mark ii benchmark experiment. *Nuclear Energy in Central Europe'98*, page 35.

[4] Elmer E Lewis. *Fundamentals of nuclear reactor physics*. Academic Press, 2008.

[5] Ye Cheng; Jeremy A Roberts. Impact of spatical discretizations on reactivity biases in depleted triga fuel.

[6] E Fridman and J Leppänen. On the use of the serpent monte carlo code for few-group cross section generation. *Annals of Nuclear Energy*, 38(6):1399–1405, 2011.

[7] T Goorley, M James, T Booth, F Brown, J Bull, LJ Cox, J Durkee, J Elson, M Fensin, RA Forster, et al. Initial mcnp6 release overview. *Nuclear Technology*, 180(3):298–315, 2012.

[8] H Böck and M Villa. Triga reactor characteristics, 2004.

[9] *Training Manual Kansas State University Nuclear Reactor Facility License R-88 Docket 50-188*.

[10] WL Whittemore, WA Stout, JR Shoptaugh, and RH Chesworth. Operation and maintenance experience at the general atomic company's triga reactor facility at san diego, california. Technical report, 1982.

[11] M. Ravnik S.Slavic, B. Zefran. Wims-d/4 for pc at 386 computer. Technical report, J. Stefan, 1990.

[12] M. Ravnik A. Trkov. Trigap, a computer program for research reactor calculations. *Nuclear Society of Slovenia*, 1985.

[13] Matjaž Ravnik and Irena Mele. Optimal fuel utilization in triga reactor with mixed core. 1988.

[14] A Persic and S Slavic. Triglav-a computer program for research reactor core management calculations. 1995.

[15] Timothy E Valentine. Mcnp-dsp users manual. *ORNL/TM-13334, Oak Ridge Nat. Lab*, 1997.

[16] Robert Jeraj, Tomaz Zagar, and Matjaz Ravnik. Monte carlo simulation of the triga mark ii benchmark experiment with burned fuel. *Nuclear technology*, 137(3):169–180, 2002.

[17] Douglas C Montgomery. Runger. *Applied Statistics and Probability for Engineers" John Wiley & Sons, New York*, 2003.

[18] Teresa Kulikowska. Reactor lattice transport calculations. *SMR*, 1220:2, 2014.

[19] MD DeHart. Sensitivity and parametric evaluations of significant aspects of burnup credit for pwr spent fuel packages. *ORNL/TM-12973, Lockheed Martin Energy Research Corp., Oak Ridge National Laboratory*, 1996.

Appendix A

Burnup Conversion

In this note, the consumption rate of 1.24 g of ^{235}U per MWD indicated in Section 2.2 is developed. The formulation takes into account only thermal energy cross section of ^{235}U.

$$\begin{aligned} & 1\text{MW d} \times \frac{10^6\text{W}}{1\text{MW}} \times \frac{3600\text{s}}{1\text{d}} \text{ Joules} \\ & \times \frac{1.60 \times 10^{-13}\text{MeV}}{1\text{J}} \times \frac{200}{1\text{MeV}} \text{ Fissions} \\ & \times \frac{(\sigma_f + \sigma_c)}{\sigma_f} {}^{235}\text{U atoms lost} \times \frac{235.04\text{g/mol}}{6.022 \times 10^{23}\text{atoms/mol}} \\ & = \boxed{1.24 \text{ g}} \end{aligned} \tag{A.1}$$

where $\sigma_f = 585$ b and $\sigma_c = 99$ b

Appendix B

KSU estimated fuel element burnup

Fuel ID	burnup $\frac{MWD}{kg(U)}$	σ (%)	Fuel ID	burnup $\frac{MWD}{kg(U)}$	σ (%)
6315	8.07	0.22	5018	27.22	5.81
6578	6.02	0.22	5027	26.40	5.85
6526	7.17	0.24	5021	27.04	5.42
6223	6.32	0.27	5026	27.11	4.89
6577	8.00	0.21	4339	23.29	5.78
6525	7.37	0.22	4143	40.73	6.39
6224	6.86	0.28	5022	30.96	5.45
6316	7.78	0.23	4078	49.10	6.19
6317	8.05	0.25	3684	44.63	6.97
6527	7.57	0.26	5000	32.19	5.63
6314	7.66	0.26	5031	30.71	5.67
2788	7.23	3.28	5653	32.06	5.69
3107	20.22	4.07	5654	29.84	6.14
3082	14.84	3.19	5019	29.01	6.18
2425	13.68	5.00	5039	22.25	6.65
3329	18.53	3.83	5253	35.17	6.26
4072	38.48	5.61	5254	26.95	5.22

Fuel ID	burnup $\frac{MWD}{kg(U)}$	σ (%)	Fuel ID	burnup $\frac{MWD}{kg(U)}$	σ (%)
3380	17.97	4.17	5649	27.97	4.79
3330	16.05	4.14	5256	29.78	5.38
3336	15.94	4.09	5647	31.59	6.54
2789	15.04	5.20	5655	32.17	5.01
3498	15.81	3.67	5944	32.38	5.73
3501	15.78	3.90	5950	28.36	6.85
3494	15.48	3.67	5939	33.15	5.88
3696	15.98	3.81	5946	32.46	5.47
3876	16.65	3.67	5947	29.70	6.01
2435	12.86	2.87	5948	33.19	5.95
2448	15.66	3.57	5949	31.96	5.63
2452	16.16	3.96	5951	29.58	5.76
3105	17.78	4.14	2144	2.18	0.43
3018	18.70	4.49	2900	5.34	3.55
3147	18.58	4.17	2907	5.58	3.43
3144	18.39	4.19	2909	4.58	4.12
3111	17.92	4.55	2914	6.38	2.86
3326	19.97	4.47	2917	4.33	4.44
4080	35.68	6.19	2933	5.53	3.15
2458	14.30	3.97	2934	6.73	2.75
3006	15.04	4.11	2937	2.92	6.00
3008	15.49	4.10	2942	2.95	6.35
3014	17.98	4.09	2949	4.62	4.04
3011	17.98	4.89	2953	6.83	2.82
3009	16.96	4.01	2963	7.19	2.46
3503	14.42	3.80	2966	7.79	2.42
3502	9.97	3.04	2982	2.94	7.10
3517	9.93	2.93	2986	6.78	2.53
3690	14.39	3.95	2987	5.87	3.16
3113	17.15	5.24	2988	2.96	7.08

Fuel ID	burnup $\frac{MWD}{kg(U)}$	σ (%)	Fuel ID	burnup $\frac{MWD}{kg(U)}$	σ (%)
3118	17.18	4.17	2989	2.97	6.25
4102	29.20	6.52	10706	0.20	1.08
4343	26.19	4.94	10707	2.32	0.46
4349	23.72	5.59	10893	0.22	0.96
4351	30.26	5.42	10894	0.46	0.66
4742	36.46	5.25	10895	2.36	0.46
4991	24.75	5.10	10880	2.49	0.43
4744	23.97	4.97	11341	1.26	0.50
5014	24.51	5.10	11351	2.25	0.50
5001	24.68	4.94	11352	0.00	0.00
5017	28.26	5.28			